University of Hertfordshire
UH

PROJECT REPORT

BACHELOR OF ENGINEERING IN AEROSPACE

Name: Sam Alex Anderson

Supervisor: David Germany

Conceptual Design of an Asteroid Sample Return Spacecraft

Report subtitle and date in Arial Bold 11pt

Date

*Delete and add your degree name AS APPROPRIATE!!!

Bachelor of Engineering Degree with Honours in Aerospace
Engineering with Space Technology
BEng Individual Project Report
School of Engineering and Technology
University of Hertfordshire

Conceptual Design of an Asteroid Sample Return Spacecraft

Report by
Sam Alex Anderson

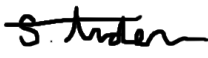Supervisor
David Germany

Date
29/03/2019

I.   DECLARATION STATEMENT

*[The heading above is set to **Heading 1** paragraph style but with the automatic number deleted. Paragraph styles need to be used consistently so that the automatically generated table of contents works correctly]*

I certify that the work submitted is my own and that any material derived or quoted from the published or unpublished work of other persons has been duly acknowledged (ref. UPR AS/C/6.1, Appendix I, Section 2 – Section on cheating and plagiarism)

Student Full Name: Sam Alex Anderson

Student Registration Number: 14165122

Signed: ……… ~~S. Anden~~ …………………
Date: ………………29/03/2019……………………...

II.   ABSTRACT

This report discusses the conceptual design of the MAIAR spacecraft intended as an asteroid sample return platform. A list of scientifically interesting asteroids was created and 4660 Nereus was chosen as the destination owing to its easy access from Earth, requiring only 5.3 km/s of delta V. Once the destination was set, the subsystems of the spacecraft were designed to comply with the requirements necessary to successfully rendezvous with Nereus and return. The subsystem design involves the analysis of the systems to their intended role. Examples of analysis performed include structural and control systems. As well as the math necessary to determine whether the system is fit for purpose. Once all the subsystems were designed they were assembled into the model for the spacecraft. The spacecraft uses two sampling methods unlike its predecessors, a diamond tipped core drill and a kinetic impact regolith collector.

III. ACKNOWLEDGEMENTS

I'd like to thank my family for the support they have given me throughout university and the push I need to succeed.

I'd like to thank my supervisor David for being a constant ray of sunshine throughout this process and allowing me to pursue the topic that really interested me.

I'd like to thank my friends for the support they've given me and my amazing girlfriend who has been so understanding throughout.

IV.   TABLE OF CONTENTS

1. INTRODUCTION

1.1 Aims and Objectives

This section lists the aims and objectives of the project and provide the framework

Aims:

1. *To produce a conceptual design for an asteroid sample return spacecraft.*

2. *To establish a viable mission profile for the spacecraft.*

Objectives:

1. *To specify a mission profile comprising trajectories, potential target asteroids and launching of the spacecraft.*

2. *To identify and select key technologies necessary for use on an asteroid sampling spacecraft.*

3. *To facilitate the integration of necessary subsystems into a functioning spacecraft that meets requirements.*

4. *To evaluate the capacity of the spacecraft against the requirements and mission profile to assess its suitability for task.*

1.2 Asteroids

The asteroids are among some of the oldest celestial bodies in the solar system, meaning they have incredible scientific value. They give a snapshot of the solar system's formation and composition. However asteroids are not homogenous; they have various different compositions and their formation occurred at different times and locations. Therefore in order to gain a true understanding of the early solar system clearly a large sample size is necessary. Asteroids are conventionally classified using the Tholen or SMASSII systems -which categorise the asteroids by spectral type- and by orbital characteristics which places them into 'families' based on their shared orbital parameters.

One such group is the Near Earth Asteroids (NEOs) which is typically subdivided into three families: the Apollos, the Amors and the Atens. These groups of asteroids are also known as Earth-crossing asteroids making them an ideal target for missions. They are thought to be main belt asteroids that have been pulled into the inner solar system. This allows the study of main belt asteroids without the extra requirements necessary for a spacecraft to access the main belt.

Having identified an easy target group of asteroids, attention can be paid to a target spectral type. The three most common asteroid types are C, S and M classes according to the Tholen classification system -in order of most to least common. Type C asteroids or carbonaceous asteroids represent 75% of all known asteroids. They are characterised by their relatively high concentration of carbon present in their composition. Water is also been identified on these asteroids which makes them scientifically valuable. Type S asteroids make up around 17% of all known asteroids and their composition is siliceous. They also contain metals, including rare Earth metals making them interesting from an economic and industrial standpoint. Finally type M asteroids are composed almost entirely of metals, as much as ten times more than type S. This makes them highly valuable. They are also much less understood due to their relative rarity compared to the other two classes.

1.3   Sample Return

There are examples of past and current sample return missions to draw from, the most prominent of which is the apollo program. "Between 1969 and 1972 six Apollo missions brought back 382 kilograms (842 pounds) of lunar rocks, core samples, pebbles, sand and dust from the lunar surface." [1]. Fully autonomous sample return has also been successful, with the stardust mission returning samples from a comet's coma. Two key programs that will be made reference in this report are JAXA's Hayabusa missions and NASA's Osiris-REx mission. Both of these programs have asteroids as their sample target. These missions both focus primarily on the search for organic molecules to ascertain the origin of life; as well as to better understand the early evolution of the solar system.

These missions

1.4   Technology

The space industry is dynamic and quick to accept new emerging technologies due to the high levels research being undertaken. Because the budgets for space missions are large and the spacecraft themselves unique; more advanced and expensive technology can be employed. The space industry has a long history of finding terrestrial applications for the technology it develops for space travel. Propulsion, power generation and battery technology are but a few examples of advances that are allowing spacecraft larger operational scopes than ever before. Electric propulsion for example has seen a hundred-fold increase in thrust, its utility evolving from purely satellite attitude control and autonomous probes to possible human spaceflight.

1.5   Purpose

Asteroids act as time capsules of the early solar system, making them valuable scientific targets. Different types and locations of asteroids are needed to give the whole picture as to the formation of the solar system. For example, type M asteroids are thought to originate from the cores of protoplanets; while type E asteroids are thought to originate from the crust. The different spectral types and locations are discussed further in section 2.1. Though it can be seen how many sample return missions would be needed to create a model of the young solar system.

As well as the scientific value of asteroids, there is also financial value. Asteroids contain higher concentrations of rare Earth metals than can be found in the crust of the Earth. Type X asteroids are largely metallic and so have a yet higher concentration of these elements, as well as metals such as iron and nickel. These materials could be mined for financial gain back on Earth, or used to build infrastructure in space. Asteroids also have been found to contain water, which can be used to manufacture rocket fuel for spacecraft. It is clear then that asteroids hold the key for the eventual colonisation of space, and it would be prudent to gain a better understanding of their composition to explore their resource utility.

Currently the composition of asteroids is based on the spectral emission of the asteroids and a few sample return missions. In order for asteroid mining to become a reality there needs to be increased understanding of composition and how this can be accurately estimated from afar; in order to judge the resources that can be utilised from them and their financial value. In this regard the scientific, financial and engineering interest in a mission of this kind all align, the composition being of vested interest to all parties.

2. **MISSION PROFILE**

2.1 Asteroid Selection

Naturally in order to tailor the specification of the spacecraft to the mission, a target must be selected. The Solar system is full of asteroids throughout and selecting a single asteroid for sample return necessitates some requirements to narrow the search field. Some of these requirements come from analysing the mission purpose and others as a logical consequence of the capabilities of current and near future technologies. These requirements are listed below.

- *Needs to be accessible to spacecraft with feasible propulsive methods.*
- *Asteroid must be of scientific value.*
- *Should be sufficient difference between target asteroid and previous sample return missions.*

With these requirements in mind, asteroids meeting these requirements can be identified. NASA's JPL small body database is an invaluable tool for evaluating candidate asteroids. The first requirement specifies that the asteroid must be accessible. Asteroids are not homogeneously spaced throughout the Solar system and are more commonly found in groups. The largest concentrations of asteroids can be found in the asteroid belt between Mars and Jupiter and also in the Kuiper belt found past Neptune. There are also smaller groups of asteroids such as the Trojan asteroids in Jupiter's lagrange points 4 & 5 (60 degrees either side); and the Near Earth Objects (Apollos, Atens and Amors) that orbit between Venus and Mars. Of all these groups, the NEO asteroids are by far the most accessible, due to their proximity to Earth. In fact all three sample return missions attempted on asteroids have targeted Apollo group asteroids.

The second and third requirements are in essence intertwined. The previous missions have sampled mainly the same types of asteroids; and so for a new mission would it would be valuable scientifically to sample an asteroid of completely a different classification. This brings up the topic of how asteroids are categorised; there are different methods of classification but the main types are the Tholen and SMASSII classification systems. These systems are based off the spectral type of the asteroids; that is, the emission spectrum to determine the composition of the surface. The table below gives the Tholen and SMASSII spectral types of the most common asteroids as well as a description of the types.

Tholen	SMASSII	Description
C	C	Carbonaceous (containing carbon). Most common type.
	Cb	Brighter carbonaceous. Thought to be remnants of the formation of the Solar system.
	Cg	Dark carbonaceous. Thought to contain higher levels of water.
S	S	Silicate asteroids. Next most common type.
M	X	Metallic asteroids. Containing iron and nickel. Thought to be from the cores of protoplanets.
E		Similar to M type but much rarer. Thought to originate from the crust of protoplanet

Figure 1. Description of asteroid spectral types. [2,3]

Of the types listed, Cg, Cb and S have been visited by previous missions. Therefore the options presented are to either select a different variant of a type that has been chosen previous, or to choose an entirely different type. The asteroid types that were not mentioned in the above table were discluded due to their rarity in the solar system; with this considered, X type asteroids stand out as being both unique in their scientific value and common enough to have a larger pool of potential targets. Their scientific value stems from the belief that they originate from shattered protoplanets. They are also of value due to their metallic composition, which has financial and engineering applications as discussed in section 1.5.

With the scope narrowed down, the JPL database can be queried for any asteroids fitting the criteria. Below is the list of potential candidates and their relevant data.

Asteroid	Classification	SMASSII Class	Semi-Major Axis	Eccentricity	Inclination	Minimum Delta V for launch within 20 years.	Arrival velocity
10302 (1989 ML)	Amor	X	1.272	0.137	4.378	4.20 km/s	3.50 km/s
2002 AK14	Apollo	V	1.017	0.106	18.018	10.10 km/s	1.00 km/s
2002 AL31	Apollo	X	1.177	0.248	7.612	6.50 km/s	4.20 km/s
15817 Lucianotesi (1994 QC)	Amor	Xc	1.325	0.118	13.872	8.40 km/s	4.10 km/s
65803 Didymos (1996 GT)	Apollo	Xk	1.644	0.384	3.409	6.30 km/s	3.40 km/s
4660 Nereus (1982 DB)	Apollo	Xe	1.489	0.360	1.432	5.00 km/s	0.30 km/s
363067 (2000 CO101)	Apollo	Xk	1.076	0.090	15.322	8.00 km/s	6.20 km/s
85990 (1999 JV6)	Apollo	Xk	1.008	0.311	5.319	6.60 km/s	4.10 km/s
35396 (1997 XF11)	Apollo	Xk	1.443	0.484	4.099	8.40 km/s	2.70 km/s
152563 (1992 BF)	Aten	Xc	0.908	0.272	7.255	6.30 km/s	5.00 km/s
2002 DO3	Apollo	X	1.860	0.499	3.801	7.40 km/s	1.00 km/s
194006 (2001 SG10)	Apollo	X	1.449	0.424	4.257	7.60 km/s	2.30 km/s
48603 (1995 BC2)	Amor	X	1.917	0.430	5.025	7.80 km/s	4.30 km/s
17511 (1992 QN)	Apollo	X	1.190	0.359	9.582	7.40 km/s	3.90 km/s
7474 (1992 TC)	Amor	X	1.566	0.292	7.088	7.00 km/s	3.40 km/s

Figure 2. Data for asteroids fitting the requirements.

The most important information tabled here are is the delta V and arrival speeds. This directly correlates to how much fuel is needed to arrive at the asteroid and be captured by it respectively. The prominent choice here is 4660 Nereus which has the lowest delta V of all the asteroids. This makes it by far the easiest to arrive at. It also has the added benefit of having a small arrival velocity meaning that the spacecraft doesn't have to burn much fuel to enter into orbit around the asteroid. The clear choice for the mission is then 4660 Nereus, with 10302 (1989 ML) serving as an alternate choice. The low delta V requirements relies on the relative positions of the Earth and the asteroid. This brings about the topic of transfer windows; which are the window of opportunity to launch during which the delta V requirements are lower. There are two main transfer windows for 4660 Nereus, the first transfer window is open between 2018 and 2021. The second transfer window is open between 2029 and 2032. Because the first transfer window is currently open at the time of this report it will be discounted; due to the time taken to develop and construct the spacecraft, the transfer window will have closed by the time the spacecraft is done. Therefore the transfer window selected is around 2031. As speculated in section 1.4 this allows for near future technology to be considered for the spacecraft design.

2.2 Launch

The launching of the spacecraft is one of the most extreme phases of the whole mission. Having to endure G-forces in excess of 20G, high vibrational modes and decreasing air density until vacuum. There are several launch vehicles currently in operation and more still planned for entry into service in the timeframe of the mission. Some of these vehicles transport the spacecraft into Earth orbit while others have the capability to send spacecraft further out into the solar system. For each vehicle there is an associated mass that it can lift into orbit. The table below details the possible launch vehicles.

Launch Vehicle	Payload Mass to Low Earth Orbit	Payload Mass to 4660 Nereus	Entry into Service	Launch Cost
Atlas V	20,520.00 kg	2,710.00 kg	2002	£84M ($110M)
Falcon Heavy	63,800.00 kg	6,250.00 kg	2018	£69M ($90M)
Delta IV-H	28,790.00 kg	6,860.00 kg	2004	£125M ($164M)
SLS-2	130,000.00 kg	32,805.00 kg	2029	£765M ($1B) est.
SLS-1B	95,000.00 kg	12,310.00 kg	2024	£765M ($1B) est.

Figure 3. Specification of launch vehicles.

The table suggests that the selection of a launch vehicle is a multifaceted problem. Judging purely based on the payload mass the Space Launch System seems the more attractive option. The Falcon Heavy launcher has the lowest launch cost due to the reusability of the launcher. Looking at all of these options as a whole, the Falcon Heavy and Atlas V present the best options for the launching of the spacecraft; which will likely not come close to the maximum payload mass of the launchers. The Atlas V having been in service for such a long time can be assumed to be very reliable. While the Falcon Heavy presents a financial and environmental advantage as a launch platform because of its reusability.

2.3 Earth Escape and Coast to Asteroid

Because the selected launch platforms are capable of sending the spacecraft directly to the asteroid without it having to use its own engines this saves onboard fuel for other maneuvers. There will likely still need to be small correction burns as the spacecraft coasts towards the asteroid which can be handled by the spacecraft thrusters. During this stage of the flight however the spacecraft will be dormant for a large portion. Hibernation can be employed to save

resources for when they are needed. As the spacecraft coasts away from the Sun, the solar panel power generation will decrease and so hibernation accounts for this decrease when systems are not needed.

The orientation of the spacecraft needs to be maintained during this period in order to keep the solar panels pointed towards the Sun and the communication array pointed towards the Earth. There are passive methods of maintaining a Sun-facing attitude using momentum wheels and solar radiation pressure. This will likely be employed during this phase of the mission to save on attitude control fuel. Once the spacecraft begins to approach the asteroid, it will awaken and begin to image the asteroid.

2.4   Asteroid Rendezvous and Orbit

At a sufficient distance from the asteroid the rendezvous maneuver can begin. The spacecraft fully wakes from hibernation and begins the steps for capture. The scientific instruments begin scanning the asteroid's topology. In order to be captured by the asteroid the spacecraft needs to cancel out its relative velocity to the asteroid. According to figure 2 the relative velocity between 4660 Nereus and the spacecraft is 0.3 km/s. This needs to be brought to zero by performing a retrograde burn. Once the maneuver has been completed the spacecraft will start drifting towards the asteroid, accelerated by its small gravity. The asteroid is not a sphere and therefore does not have a uniform gravity across its surface, therefore one of the first scientific and practical investigations of the spacecraft is to determine the gravitational profile of the asteroid. This can be achieved by the knowledge that once in orbit around the asteroid the spacecraft will orbit the centre of mass. Using the laser altimeter the spacecraft can determine the location of the centre of mass relative to the surface features and thereby determine an optimum orbit to maintain.

Once the spacecraft is in a stable orbit around the asteroid, scientific observation can be started proper. The nature of these observations will be discussed in section 3.8 when discussing the scientific payload of the spacecraft. Once these observations have concluded the sampling maneuvers can begin. In total there are eight of these maneuvers, four surface samples and four core samples. This requires the spacecraft to drop out of orbit around the asteroid and descend to the surface. Because of the weak gravity of the asteroid, the spacecraft can maintain a hover above the surface while the samples are taken. The exact method of the sampling maneuvers will be discussed in section 3.9. After each sample is taken, the spacecraft will retreat back into orbit and locate the next sample site.

2.5   Asteroid Escape and Earth Flyby

Once all the samples are acquired and all the data has been gathered the spacecraft must make preparations to leave the asteroid and return to Earth. Important to note is that the spacecraft does not need to re-enter Earth's orbit, only to perform a flyby maneuver. The exact details of the trajectory to return to Earth are complex and would require extensive and intensive calculation to optimise the return. The simplest return case would be where the asteroid is at aphelion. Then a Hohmann transfer maneuver can be used to transfer from the asteroid. A Hohmann transfer orbit is the most efficient transfer type when the difference between the radii of the orbits is below 12. A diagrammatic explanation of this maneuver is displayed below.

The red line indicates the original orbit, blue indicates new orbit and green indicates transfer orbit. Coloured arrows show orbit direction and black arrows indicate direction of burn.
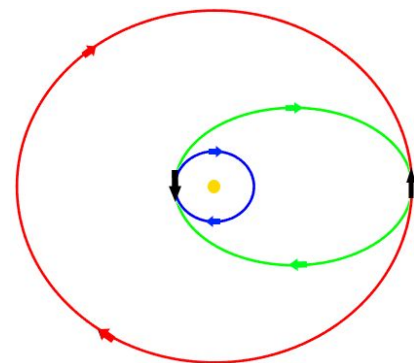

Figure 4. Diagram of a Hohmann transfer maneuver.

This method of orbital transfer would likely be unsuitable for the return as there is no need to perform the second burn. The atmosphere can be used to slow the re-entry vehicle in a maneuver called aerobraking. When the spacecraft is approaching the Earth, the sample capsule is released and carries on to eventually enter the Earth's atmosphere while the main spacecraft burns to move its trajectory so to not enter the atmosphere.

2.6   Extended Mission

Once the sample return capsule has been released the spacecraft's mission is completed. At this point the spacecraft could be left to burn up in the atmosphere. However depending on how much fuel is left in the spacecraft, a correction burn can be carried out to prevent re-entry. From this point the spacecraft will undergo a flyby maneuver where the spacecraft falls towards the planet and is accelerated by its gravity, thereby changing the spacecraft's orbit. This can be utilised to propel the spacecraft toward a new target. The potential targets would have to be decided closer to this point as it would be highly dependant on the location of the spacecraft and the fuel remaining. Potential targets would include other NEO asteroids or objects in the asteroid belt. No sampling would be able to be undertaken, but the scientific equipment would still be able to send back data. Therefore multiple flybys of other objects could be performed.

3. **SUBSYSTEM DESIGN**

3.1 *Propulsion* [4,5,6]

The method of propulsion dictates a lot of the other features of the spacecraft. Chemical thrusters require much more fuel and so the majority of the spacecraft mass would be taken up by fuel. Electric engines on the other hand require less fuel but a much greater power requirement. The table below gives the performance data for suitable thrusters.

Propulsor	Thrust	ISP	Exhaust Velocity	Description
BHT-8000	449E-03 N	2,210.00 s	21.68 km/s	8kW Hall effect thruster. Produced by Busek.
NEXT-C	236E-03 N	4,190.00 s	41.10 km/s	Next generation ion thruster developed by NASA.
NSTAR	092E-03 N	3,100.00 s	30.41 km/s	Current generation ion thruster produced by NASA.
AEPS	589E-03 N	2,600.00 s	25.51 km/s	Next generation Hall effect thruster developed by NASA.
R-6D	022E+00 N	294.00 s	2.88 km/s	Bipropellant chemical thruster produced by Aerojet.
HiPat	445E+00 N	329.00 s	3.23 km/s	High thrust liquid thruster produced by Aerojet.
XIPS-25	165E-03 N	3,500.00 s	34.34 km/s	Current generation ion thruster produced by L-3 Communications.

Figure 5. Thruster specifications for selection.

Judging from this table there is a clear choice to make first and foremost; whether to use chemical or electric thrusters. Chemical thrusters have higher thrusts than electric thruster but lose out on efficiency where electric engines have the edge. There is another consideration to make, as the spacecraft will be required to hover above the asteroid surface, the exhaust should contribute as little contamination of the samples as possible. With electric engines this is straightforward as they use propellants that would not naturally occur on the surface of the asteroid and that are not being searched for in the samples. Chemical engines however potentially do have contaminants in their exhausts; Liquid oxygen and liquid hydrogen for example react to form water, which is one of the compounds that is being searched for on the asteroid. Ultimately the deciding factor will be if the fuel and power requirements for the spacecraft can be met using each of these thruster types. The table below shows how much fuel would be needed relative to the total mass for each thruster, assuming a delta V for return equal to that to arrive.

Propulsor	Propellant Mass Ratio	Fuel Fraction
BHT-8000	1.31	23.83%
NEXT-C	1.15	13.37%
NSTAR	1.21	17.63%
AEPS	1.26	20.65%
R-6D	7.73	87.07%
HiPat	6.22	83.93%
XIPS-25	1.19	15.79%

Figure 6. Calculated performance with thruster.

The table shows that in order to use chemical rockets to propel the spacecraft, 80% of its mass must be fuel. Therefore electric engines as a whole present a much more attractive option. The NEXT-C thruster in particular shows great promise as a propulsive method; with relatively high thrust for an ion engine as well as high efficiency. Below is the technical data available for the NEXT-C thruster. The thruster is still under development and these values are subject to change.

NEXT-C Ion Thruster	
Thrust (Minimum to Maximum Throttle)	17.1 mN to 236.0 mN
Maximum Specific Impulse	4190 s
Power Draw at Maximum Throttle	6.9 kW
Propellant Throughput	450 kg

Figure 7. Next-C specification.

NASA's NEXT-C thruster while not currently in production has been extensively tested and determined to have a throughput of 450 kg of fuel before failure. With these thrusters and a maximum throughput of 450 kg the maximum spacecraft mass is around 3365 kg. This upper bound is more than sufficient considering the launch mass of the previous missions. Adding a second thruster can double the maximum spacecraft mass; and also provides redundancy in the event of a thruster failure. As stated previously, electric thrusters' limiting factor is power consumption rather than available fuel. At maximum throttle the NEXT-C thruster draws 7 kW of power. Two of these operating simultaneously would draw 14 kW, which is a substantial amount power that needs to be generated. The next section will discuss the power generation capabilities of the spacecraft in more detail.

As the chosen thruster is currently in development, the dimensions are largely unavailable. Only one dimension is currently available and so pixel measurement techniques were employed to develop the computer aided designs shown below. The first design shows the NEXT-C thruster while the second shows the nest of two thrusters.
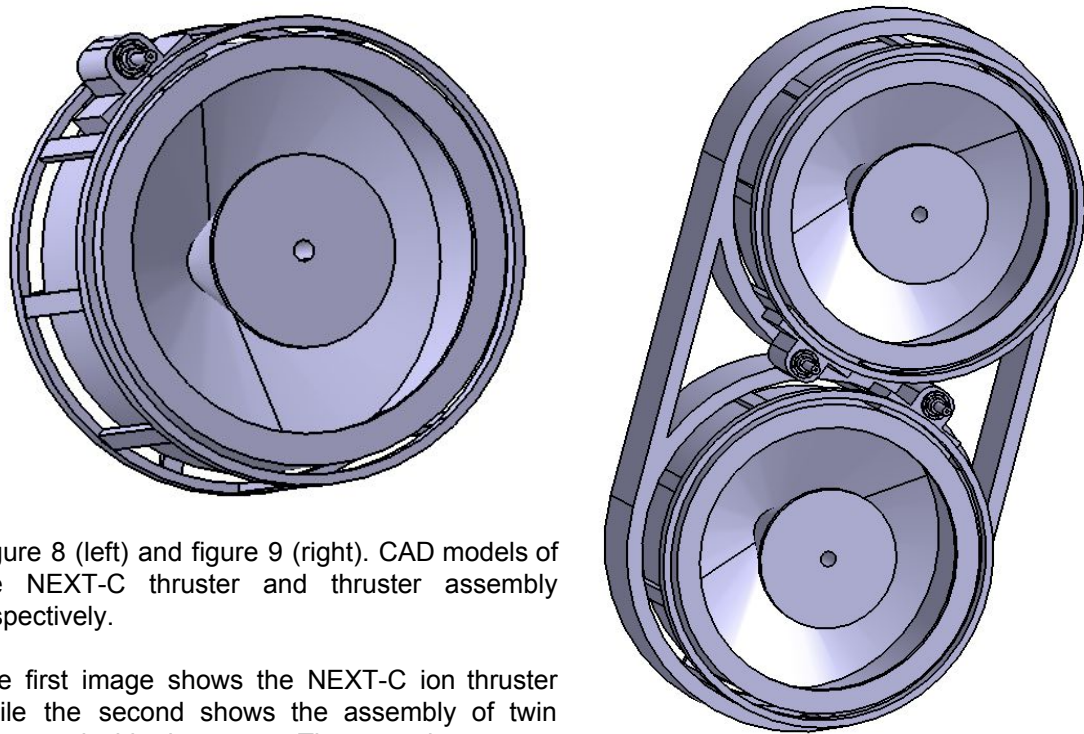
Figure 8 (left) and figure 9 (right). CAD models of the NEXT-C thruster and thruster assembly respectively.

The first image shows the NEXT-C ion thruster while the second shows the assembly of twin thrusters inside the mount. The mounting system places the two thrusters close enough so that the neutraliser found in the top left of the first image can service both thrusters in the event of failure. The mount is made from aluminium and acts to bolt the thrusters to the structure.

3.2   Power [7,8,9,10, 11]

Having chosen an electric propulsion system, clearly power generation is a key factor in the effectiveness of such a system. This section will discuss the power generation options available to the spacecraft. There are four main types of power generation available to spacecraft.

- Solar Power.
- Radiothermal Isotope Generators.
- Nuclear Reactors.
- Fuel Cells.

Solar power systems use radiated power from the Sun to convert into electrical power. This can be via solar panels or solar collectors. Panels use the photovoltaic effect to convert incident light into electrical power while solar collectors use lenses to focus the light into a point. These methods rely on direct line of sight with the Sun in order to provide power. Additionally the power recoverable diminishes with the inverse square law; meaning that the father away from the Sun the spacecraft gets, the larger the solar panels would need to be in order to generate the same power output. This indicates that at certain distances from the Sun, solar panels would have to be unfeasibly large and thus would be inadequate for such a mission.

Radiothermal Isotope Generators or RTGs use the thermal decomposition of radioactive elements in order to convert the thermal energy into electrical power. These do not rely on outside factors and typically the lifetime of these generators is measured in decades. They have the added benefit of transferring heat to warm the spacecraft without the need of radiators. RTGs however have low power outputs, meaning many would need to work in parallel to power the ion thrusters. A danger of RTGs in reference to the mission at hand it the possibility of accidental re-entry into the atmosphere; because the spacecraft would contain radioactive materials, if the spacecraft burns up in the atmosphere the area around the re-entry site could become contaminated.

Nuclear reactors function similarly to RTGs, however the radioactive decay is forced rather than passive, as such they can provide much more power than is possible with RTGs and even solar panels. They do however need a constant source of fuel and have to be managed correctly to prevent overheating and runaway reactions. They tend to be heavy due to the shielding needed to protect the scientific instruments and electronics. As well as suffering from the same problems as RTGs with regard to the environmental concerns. In general unless there is no other method to generating large amounts of power, nuclear reactors in space are discouraged.

Fuel cells function by reacting two chemicals together to generate electricity, which in the case of spacecraft tend to be the onboard fuels. Since the spacecraft is using xenon as its main propellant - which is inert and requires no chemical reaction to generate thrust - it cannot be used in a fuel cell. The monopropellant for the attitude control system could be used to run a fuel cell. However because the electricity generated by the fuel cell would go towards powering the ion thrusters the use of fuel cells becomes redundant; since more fuel would be used to generate the electricity for the thrusters than would be used by a chemical thruster in the first place. The use of fuel cells makes much more sense when used with chemical propulsion to power the other subsystems of the spacecraft.

Because the distance from the Sun that the spacecraft would deviate being no more than 1.5 AU, the use of solar panels would be adequate for powering the spacecraft. The next task is to select and size these solar panels to the needs of the spacecraft. Looking forward into the future, many advances in solar technology are being researched. Brought on in part by the interest in renewable energy. Rigid solar panels are beginning to be replaced by thin flexible panels that are able to reduce to a stowage volume many times smaller than the equivalent area of rigid panels. Such a panel has recently been tested aboard the ISS.
The table below shows how one such near future flexible panel compares to the rigid panels aboard the Hayabusa mission.

Power Generation	Power Generation (kW)	Efficiency	Area Necessary (m^2)
Inflatable solar panels	6.66	40.00%	12
	1.62	40.00%	12
Rigid Hayabusa Panels	2.6	15.62%	12
	0.634	15.62%	12

Figure 10. Calculated performance of rigid panels vs inflatable panels.

As can be seen the inflatable panels are much more efficient than the rigid panels. Because they are thinner they also have a greater specific power than the rigid panels, that is the power per unit mass. The panels will be designed to roll up to stow for launch and when free of the atmosphere unfurl using inflatable guide vanes to make the panels rigid. The design for these panels can be seen below. They will be mounted on a single axis gimbal in order to track the Sun to maintain power generation.
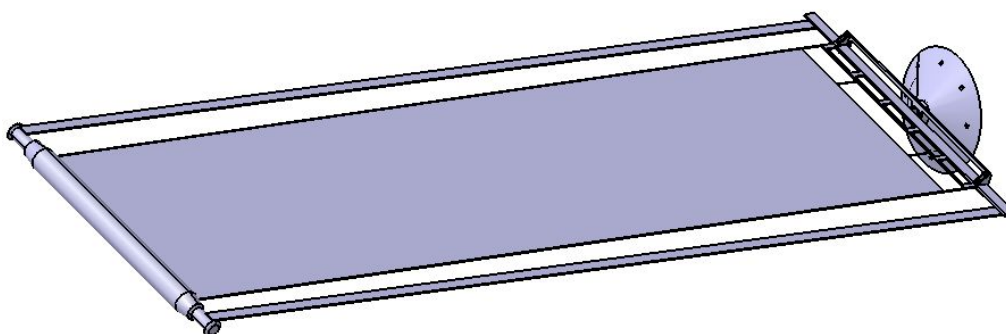

Figure 11. CAD model of solar panel assembly.

The power consumption of the spacecraft in total will be largely dominated by the ion thrusters, being the most power intensive part of the spacecraft. Appendix A shows the estimates for the power consumption of the individual components of the spacecraft. Scaling the values from the above table to a total panel are of 30m² gives an optimum power generation of 16.6 kW at 1AU which provides enough power to run both thrusters simultaneously as well as the rest of the subsystems needed for the cruise phase. This gives the panels dimensions of 2m by 7.5m each. Considering ESA's Rosetta mission used a panel area of 60m² this is entirely possible with current technology.

One of the problems facing solar panels in a space environment is cell degradation. This is caused by intense solar radiation causing the cells to lose efficiency over time. The table below shows expected degradation rates over time.

Degradation Rate (% per year)	0.80%	1 AU	1.4 AU
Initial Efficiency	40%	16.64 kW	4.06 kW
1 Year	39%	16.31 kW	3.98 kW
2 Years	38%	15.98 kW	3.90 kW
3 Years	38%	15.64 kW	3.82 kW
4 Years	37%	15.31 kW	3.73 kW
5 Years	36%	14.98 kW	3.65 kW
10 Years	32%	13.31 kW	3.25 kW

Figure 12. Calculated panel degradation over time.

As can be seen the degradation rate over a ten year period never debilitates the spacecraft from operating with at least one thruster at 1AU. Farther afield the spacecraft can throttle the thruster. There may be times throughout the mission where the solar panels are eclipsed by either a planetary body, the asteroid or the spacecraft itself. During these periods the spacecraft must rely on backup battery power to maintain its systems. These battery systems might also be used to supplement the solar power in times of high load. Battery technology is a highly researched field also, and the table below compares different battery types for application to the spacecraft.

Batteries	Energy Density	Use time	Energy Content	Battery Mass
Current Liquid Lithium Ion Batteries	260 kWh/kg	3.00 hr	14,400.00 kWh	55.38 kg
Future Liquid Lithium Ion Batteries	400 kWh/kg	3.00 hr	14,400.00 kWh	36.00 kg
Current Solid State Batteries	155 kWh/kg	3.00 hr	14,400.00 kWh	92.90 kg
Future Solid State Batteries	480 kWh/kg	3.00 hr	14,400.00 kWh	30.00 kg

Figure 13. Battery specifications.

The benchmark for which to size the batteries is to provide full cruise power for 3 hours in total eclipse. Due to the mission profile of the spacecraft it is unlikely that the spacecraft will have to operate under eclipse conditions for long periods of time. Future liquid lithium ion batteries show promising research, as the technology has come a long way, while research on solid state batteries is still in its relative infancy. For this reason the future liquid batteries will be employed on the spacecraft.

3.3 Command and Control[12]

The next step is to give the spacecraft a 'brain' in order for it to carry out tasks autonomously, while still being able to accept instruction from ground stations. Because of the distance between the asteroid and Earth (2.4 AU at aphelion) the communication times are approximately 20 minutes outgoing and 20 minutes return. A 40 minute feedback delay makes it near impossible to manually control the spacecraft. Instead instructions are sent ahead of time to the spacecraft and the spacecraft must carry out those tasks assigned to it. In the past this relied on exact timings and positions to have the spacecraft carry out the instructions correctly. Artificial intelligence (AI) could provide the spacecraft with an invaluable asset to these missions - improvisation. An intelligent spacecraft could correct for problems that occur in situ, which ground control may not know about for another 20 minutes. In close proximity to the asteroid undertaking a sampling maneuver this could be the difference between impacting the surface and successfully completing the maneuver.

AI naturally requires superior processing power than would be required to simply process instructions. Processor technology is one of the most quickly advancing technologies available with the rule of thumb being a doubling in processing power every two years. Multicore processors are now standard on the majority of home computers and allow the computer to complete a multitude of tasks simultaneously. The processors of Earth bound computers would not be suitable for space applications however, this is due to the harshness of the space environment. Intense radiation causes damage to circuits over time. To combat this problem, processors can be radiation hardened. Below is a list of current radiation hardened processors.

Name	Type	Speed	Power Consumption
RAD 5510	Single Core	1.4 GOps	11.5 Watts
RAD 5545	Multi-Core	5.6 GOps	20 Watts
RAD 750	Single Core	0.27 GOps	5 Watts

Figure 14. Specifications of spacecraft computer processors.

The RAD 5545 processor has the highest performance of all the current generation processors. There is no doubt that within the timeframe of the mission the performance will increase further.

As with all subsystems in space travel, redundancy is important in order to maintain operation despite faults. Two of the methods to provide redundancy in the computer systems are to have a completely independant computer system or to have a distributed network of processors. The independent redundant system would be inactive until the failure of the primary system, at which point it would take over as primary. The distributed network functions by having several processors spread around the spacecraft. If a fault is detected within one of the processors, the other processors can pick up the slack. Overall the distributed network provides far better redundancy as there is no delay between the failure of one system and the take up of another. It also provides multiple fault tolerance without the need of several redundant computer systems onboard.

3.4 Communication[13,14,15]

The spacecraft needs an effective method of communicating with the Earth, both for receiving commands and transmitting telemetry and scientific data. The large distances between the spacecraft and the ground necessitate the use of high gain directional antennas. There are several types of antenna with different applications, but the most fitting type is the parabolic reflector. In order to determine the size of antenna needed, first the transmission frequency must be chosen. For deep space applications there are three commonly used bands, the S band, Ku band and X band. The S band has replaced by the X band owing to the superior transmission rates. Ku band has excellent transmission rates, however depending on weather conditions can be absorbed by the atmosphere.

- S Band. 2-4 GHz.
- Ku Band. 12-18 GHz.
- X Band. 7-11.2 GHz.

NASA's Deep Space Network (DSN) operates using the X band for deep space missions. And so taking a frequency within the X band of 9.0 GHz, the required antenna dish size can be found using equation 1: $G = 10log_{10}(\eta(\frac{\pi D}{\lambda})^2)$. Where G is the antenna gain, nu is the efficiency which for a parabolic antenna can be assumed to be 55%, D is the dish diameter and lambda is the wavelength of the signal. The graph below shows how the gain changes with antenna diameter.

Because of the logarithmic nature of the function, increasing the diameter results in marginal increases in gain. Between 1.5 and 2 meter the gain only increases by 2.5 dB. Therefore the added weight and complexity from using a larger dish does not justify the increase in gain. The calculations below will determine whether a 1.5 meter dish is fit for purpose. These calculations will find the signal to noise ratio and the data transfer rate for dishes of diameter 1.5 and 2 meter.
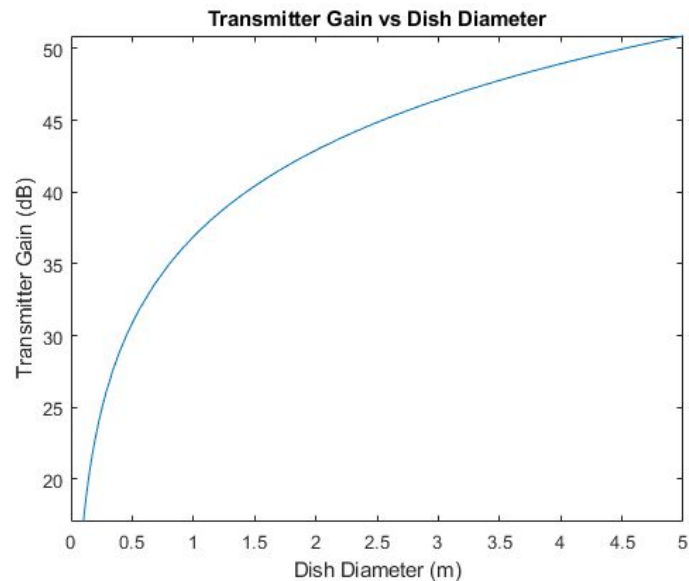

Figure 15. Transmitter gain vs dish diameter.

Dish Diameter	Signal to Noise Ratio	Data Transfer Rate
1.5 m	17.05	52 kBs / 417 kbs
2.0 m	30.31	62 kBs / 497 kbs

Figure 16. Calculated specification of communication system for 3 dish diameters.

As can be seen from the table, there is a stark difference between the signal to noise ratios, both ratios are highly suitable as they are both high enough that the signal should always be discernible. The data transfer rates are similar across the two diameters. This indicates that a 1.5 meter antenna would be suitable for the purpose and the extra mass, power consumption and complexity associated with a larger antenna does not justify the marginal increase in performance.

Now that the diameter of the antenna has been decided, the rest of the antenna can be designed. Using relationships between the diameter, focal length, depth and efficiency the optimum design can be found. The following equations 2 and 3 allow the calculation of the key design elements of the parabolic antenna. $\eta = \frac{f}{D}$ and $f = \frac{D^2}{16d}$. Where η is efficiency, f is focal length, D is diameter and d is depth. Solving the equations using known values for diameter and efficiency gives the design for the parabolic reflector shown below.
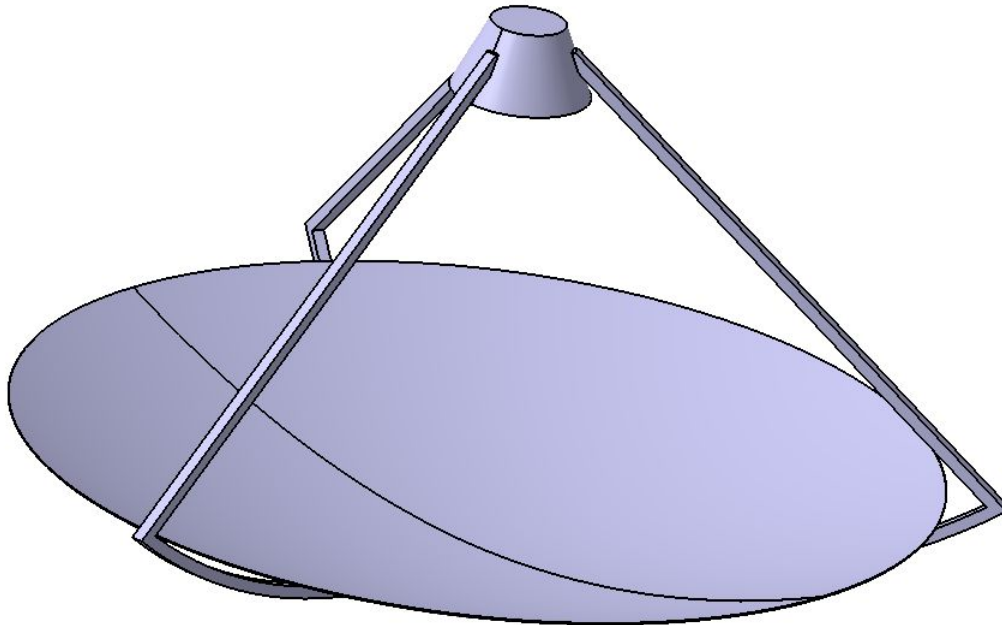
Figure 17. CAD model of high gain parabolic antenna.

Because the antenna is directional, it must be pointed towards the Earth in order to transmit data. The DSN has receivers located 120 degrees apart so to cover the entire sky regardless of the rotation of the Earth and the position of the spacecraft. The orientation of the spacecraft and by extension the antenna can be controlled by the attitude control system; however as will be discussed later, due to the external torques applied to the spacecraft the attitude control system can only control the orientation to a precision of ± 0.1 degrees. This is unsuitable as at the maximum distance the Earth's angular diameter is 0.0041 degrees or 14.64 arcseconds. For reference this is approximately the average size of Mars in the night sky. Clearly then the antenna needs the ability to be pointed independently from the main spacecraft. Implementing a two axis gimbal allows the antenna to be directed towards the Earth so long as the spacecraft is pointed in the general direction of the Earth. Herein lies a problem with the system. If the spacecraft were to encounter a problem while the spacecraft was not pointed towards the Earth, there would be no way to communicate with the spacecraft. This is where the utility of omnidirectional antenna becomes apparent. The use of two omnidirectional antennas placed at 90 degrees to the main dish and 180 degrees from each other would provide total coverage irrespective of the orientation of the spacecraft. This means that in the event of an problem occurring when the main dish is pointed away from the Earth, communication can be maintained - albeit at a much slower rate - with the ground stations.

3.5 Attitude Control[16,17,18]

Attitude control is the method by which the orientation of the spacecraft is controller. There are several methods to achieve this, some of which apply to this spacecraft, others which do not.
- Attitude Control Thrusters.
- Reaction Wheels.
- Momentum Wheels.
- Magnetic Torquer.
- Gravity Gradient Torquer.
- Solar Radiation Torquer.

Attitude control thrusters provide a torque to the spacecraft by creating thrust offset from the central axis of the spacecraft, thus creating a turning moment. They can provide large torques, but do have the disadvantages of requiring fuel, is a toggleable system so is not throttleable and can have contaminants in the exhaust plume.

Reaction wheels and momentum wheels are similar in operation and both work via the principle of conservation of angular momentum. Reaction wheels function by spinning a mass in the opposite direction to the intended direction of the spacecraft, which in order to keep the angular momentum of the whole system zero must spin in the opposite direction. The inoperative state of a reaction wheel is that of a zero angular velocity; while the momentum wheel's inoperative state has a non zero angular velocity. Therefore the momentum wheel is able to store momentum. The constant spinning state provides stability along the axis of the spacecraft via the gyroscopic effect. The disadvantage of momentum wheels is that they can become saturated when they can no longer spin any faster. Once the wheels become saturated an external torquer such as attitude control thrusters are needed to despin the wheels.

Magnetic and gravity gradient torquers operate using the local gravitational and magnetic fields to 'push' against. These are typically used for much smaller satellites and only work when orbiting an object such as the Earth, with a large gravitational and magnetic field. Solar radiation torque can be used on satellites with orientable panels from which to 'bounce' the incoming solar radiation from. For large satellites this torque is very small, but if used in conjunction with other torquers such as momentum wheels can provide a passive method of attitude control.

For this spacecraft a combination of momentum wheels, attitude control thrusters and solar radiation torque will be used to control the attitude of the spacecraft. With the momentum wheels providing the majority of the control authority and the thrusters acting to despin the momentum wheels when necessary. Momentum wheels can also double as reaction wheels should the situation require. Because the spacecraft is only using thrusters sparingly there need not be much fuel onboard for them. The specifics of the thrusters will decide how much fuel is needed. There is the choice of whether to use monopropellant or bipropellant systems. The table below discusses the different fuels available and their applicability to the spacecraft. The placement of RCS thrusters would have to be determined, but the number should be no greater than 16 as this would be enough to cover all faces with two thrusters and cover all degrees of rotation. Analytical methods can then be used to balance the spacecraft and reduce the number down further.

Sizing the momentum wheels will be done by creating a Simulink model to judge the response of the attitude control system using data from operational momentum wheels. The wheels being used are modelled after the Rockwell Collins RSI50-220/45 wheels [18]. The simulink model can be found below. Each part will be explained and the time response plotted.
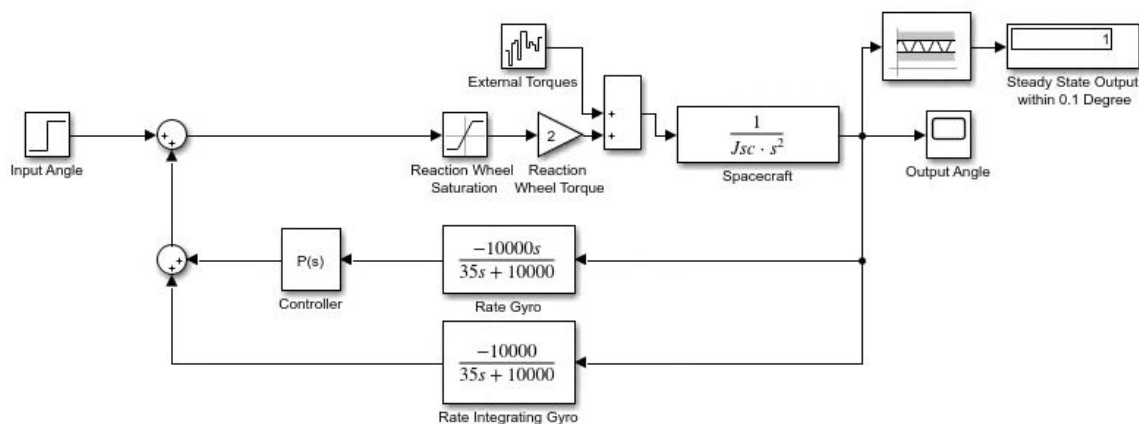

Figure 18. Simulink model describing the orientation of the spacecraft.

The model above models how the spacecraft attitude control system responds to a step input. The reaction wheel used has a saturation limiter so to simulate the saturation a reaction wheel would undergo in normal operation. External torques have been added to the system to account for external factors such as solar radiation torque. The rate and rate integrating gyros give feedback to the system. The controller in the feedback is a simple proportional controller with a gain value of 26 as this provides the best response to the system. the steady state output window checks that the steady state output stays within 0.1 degrees of the input angle, because

there is random noise in the system this value will not maintain a steady state and instead must be kept within an acceptable error range. Below is the response of the system in the time domain.
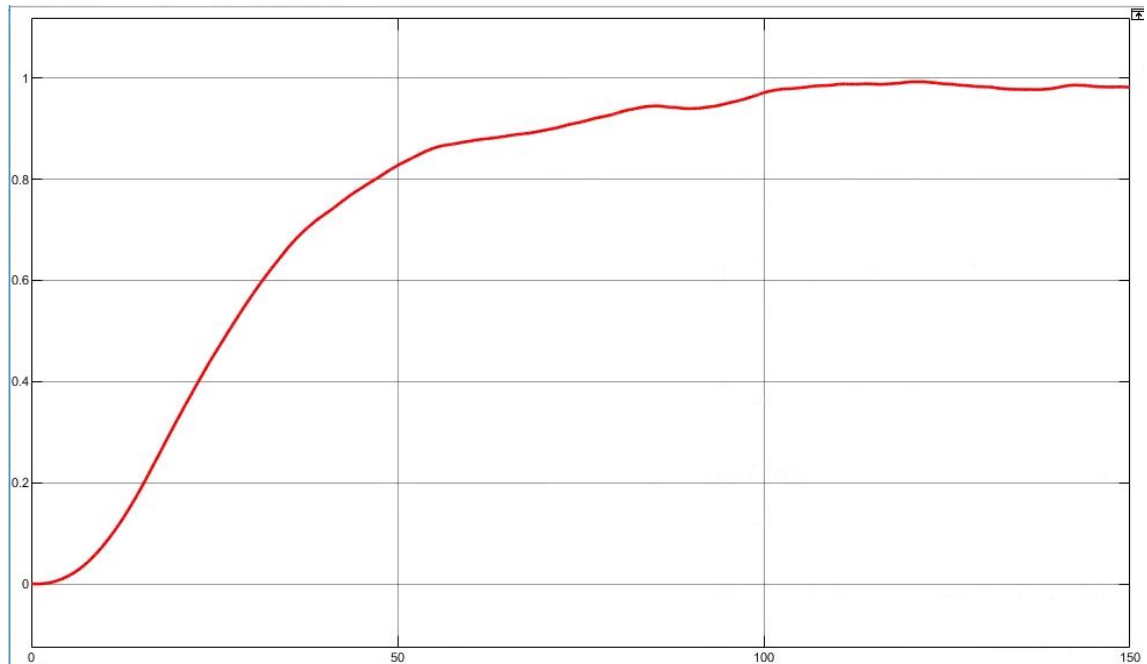

Figure 19. The step response of the system modeled above.

There are two types of gyroscope necessary to control the spacecraft attitude, a rate gyro and a rate integrating gyro. The rate gyro outputs the angular velocity of the spacecraft and when used in combination with the rate integrating gyro gives a fast response which is necessary to control this system. One last component is needed in order to form the navigational system of the spacecraft. This is the star mapper, which is responsible for chatting the stars and constellations that it can see and relating this to the orientation to give a map of the orientation of the spacecraft relative to fixed reference points.

As can be seen the response of the system is stable, indicating the reaction wheel used is suitable for controlling the spacecraft. A more powerful reaction wheel may reduce the time taken to reach steady state. The RCS thrusters can also be used to supplement the torque of the momentum wheels if necessary. The key criterion which will decide the design of the RCS thruster system is the fuel that it will use. This will impact the mass and complexity of the system. Below is a table showing various fuels and their properties. The specific impulse is a measure of how efficient the fuels are. Higher Isp's require less fuel for the same delta V. Hypergolic fuels initiate a reaction on contact and do not require any kind of ignitor. This reduces the complexity and mass.

Oxidiser	Fuel	Mixture Ratio	Specific Impulse	Hypergolic
Bi-Propellants				
Liquid Fluorine	Hydrazine	6.00	338.00 s	TRUE
FLOX-70	Kerosene	3.80	320.00 s	TRUE
Nitrogen Tetroxide	Kerosene	3.53	267.00 s	FALSE
	Hydrazine	1.08	286.00 s	TRUE
	MMH	1.73	280.00 s	TRUE
	UDMH	2.10	277.00 s	TRUE
	Aerozine	1.59	280.00 s	TRUE
Red Fuming Nitric Acid	Kerosene	4.42	256.00 s	FALSE
	Hydrazine	1.28	276.00 s	TRUE
	MMH	2.13	269.00 s	TRUE
	UDMH	2.60	266.00 s	TRUE
	Aerozine	1.94	270.00 s	TRUE
Hydrogen Peroxide	Kerosene	7.84	258.00 s	FALSE
	Hydrazine	2.15	269.00 s	TRUE
Chlorine Pentafluoride	Hydrazine	2.12	297.00 s	TRUE
Monopropellants				
Hydrazine	N/A		234.00 s	TRUE
Hydrogen Peroxide	N/A		161.00 s	TRUE
Nitromethane	N/A		276.00 s	TRUE
Nitrous Oxide	N/A		180.00 s	TRUE

Figure 20. Specification of RCS thruster propellants.

Monopropellants while having a lower specific impulse (ISP) than bipropellant systems do remove much of the complexity. A single fuel tank and fuel feed system can be used reducing the overall weight of the system. As the thrusters will only be used to despin the control wheels, monopropellants are the better choice. Hydrazine is by far the most used monopropellant, having a high ISP just below the bipropellants. The winner among the monopropellants is definitely Nitromethane. Research into nitromethane is still in its infancy, but has promise due to its high specific impulse and environmental benefits. Some of the propellants which on the surface seem like ideal fuels turn out to be completely unsuitable. One good example of this is the use of liquid fluorine as an oxidiser. At a glance liquid fluorine has excellent an specific impulse that would make it a good propellant, however it is such a good oxidiser than it cannot be stored using most materials. The table below adds another angle on what fuels are suitable for the mission by discussing at what temperatures the fuels must be kept.

Chemical	Melting Point	Boiling Point
Liquid Fluorine	-219.60°C	-188.10°C
Nitrogen Tetroxide	-9.30°C	21.15°C
IRFNA	-41.60°C	83.00°C
Hydrogen Peroxide	-0.40°C	150.20°C
Chlorine Pentafluoride	-103.00°C	-88.50°C
Kerosene	-9.60°C	216.30°C
Hydrazine	1.40°C	113.50°C
MMH	-52.40°C	87.50°C
UDMH	-58.00°C	63.90°C
Nitromethane	-28.38°C	101.19°C
Nitrous Oxide	-90.86°C	-88.48°C

Figure 20. Thermal range of RCS fuels.

The green cells indicate fuels that can be stored between -20 degrees Celsius and 50 degrees Celsius. Outside of this temperature range the thermal control of the spacecraft would get complex and energy intensive. Cross referencing the two tables again reveals Nitromethane to be an ideal fuel. The RCS thrusters require balancing to find an optimum configuration to provide three axis control for the spacecraft. The number of thrusters necessary is part of that optimisation but should be no more than 16 as this amount provides two thruster per face and gives total three axis control. With optimisation this number can be reduced.

3.6   Thermal Control[19]

The majority of the components onboard the spacecraft must be maintained at a specific temperature to remain functional. The thermal control system of the spacecraft acts to maintain the internal temperature inside a threshold for a range of external conditions. There are passive and active thermal control systems. Active systems use spacecraft power to heat or cool the spacecraft while passive systems rely on the thermal properties of the spacecraft itself to maintain a working temperature. The table below gives examples of the thermal ranges of key components onboard the spacecraft.

Component	Min Temp	Max Temp
Power Processing Unit	-10.00 °C	40.00 °C
NEXT-C Thruster	-10.00 °C	40.00 °C
Computers	-5.00 °C	40.00 °C
Solar Panels	-60.00 °C	55.00 °C
Batteries	-5.00 °C	15.00 °C
Momentum Wheels	-20.00 °C	40.00 °C
RCS Fuel	-28.38 °C	101.19 °C

Figure 22. Thermal range of components.

The batteries here present the limiting component that sets the temperature range for the spacecraft of -5°C to 15°C. A list of thermal management solutions is presented below.
- Passive systems.
    - Paints and coverings.
    - Thermal fillers and washers.
    - Mirrors to reflect incoming radiation.
    - Radioisotope heater.
- Active systems.
    - Radiators.
    - Heaters
    - Fluid pipes for heat transport.
    - Variable-emittance infrared electrochromatic skin (VIES)

Paints, coverings, mirrors and skins all work to change the emissivity and absorption values of the spacecraft exterior. Thus changing how much of the incoming radiation the spacecraft absorbs. VIES functions by using electricity to change the shade of the external skin, and thus its emissivity value. Radioisotope heaters use radioactive decay - of which heat is a byproduct - to heat a spacecraft without the need of power input. Radiators and heaters both use power to remove and add heat respectively to the spacecraft. Fluid pipes use pumps and heat sinks to move heat from hot areas to cooler areas. VIES is an emerging technology which shows great promise to allow semi-passive thermal management. The spacecraft emissivity can be varied from 0.19 to 0.9 using just 12 Watts of power to cover the whole spacecraft exterior. This makes it well suited to managing the temperature across the range of external conditions the spacecraft may encounter.

External Condition	Low Emissivity	High Emissivity
Earth		
Illuminated	106 °C	-10 °C
Eclipsed	-91 °C	-113 °C
Asteroid		
Illuminated	5 °C	-78 °C
Eclipsed	-105 °C	-135 °C
Solar Orbit		
Low (1 AU)	95 °C	-24 °C
High (1.4 AU)	-9 °C	-94 °C

External Condition	Low Emissivity	High Emissivity
Earth		
Illuminated	125.28 °C	2.20 °C
Eclipsed	-0.63 °C	-73.37 °C
Asteroid		
Illuminated	46.02 °C	-52.14 °C
Eclipsed	-4.36 °C	-83.39 °C
Solar Orbit		
Low (1 AU)	115.18 °C	-9.92 °C
High (1.4 AU)	37.45 °C	-62.61 °C

Figure 23. Thermal performance with no heaters (left) and a 4.5 kW heater (right).

These two tables show how the variable emittance skin performs both alone (left) and in combination with a 4.5 kW heater (right). From the left table it is clear that the VIES system can maintain the spacecraft temperature at acceptable levels unless eclipsed by either the Earth or the asteroid. The inclusion of a 4.5 kW heater allows the spacecraft to thermoregulate when eclipsed. It is worthy of note however that the spacecraft would likely not spend much time eclipsed as its trajectory does not require it to orbit the Earth. The asteroid would eclipse the spacecraft for short durations during which the spacecraft would not have sufficient time to cool down and therefore would not need such a powerful heater. These calculations take into account the solar radiation both direct from the Sun and reflected by the primary body (known as albedo radiation) as well as the heat radiated from the primary body. Some simplifying assumptions have been used such as assuming the orientation of the spacecraft relative to the Sun and primary body. These assumptions amount to the worst case scenarios and in actual operation the thermal ranges would not be this drastic.

3.7   Structure[20,21,22]

The structure of the spacecraft is the hardpoint to which all of the other subsystems are attached. It is also responsible for bearing the brunt of the forces that the spacecraft must endure; especially during launch. There are three types of structure that will be discussed here; substructure, superstructure and auxiliary structures. This section will discuss those three structures, demonstrate the suitability of those structures using finite element analysis (FEA) and explore the material and manufacturing considerations for each structure.

The substructure provides the base upon which the entire spacecraft is built. It transfers all the loads that act on the spacecraft and therefore needs to be rigid to hold the spacecraft together. The figure 24 shows the design for the substructure of the spacecraft. The general form of the spacecraft is that of a rectangular prism with dimensions 1.5 m x 1.5 m x 2.0 m. Running through the middle of the substructure is a pylon that acts as both a strengthening girder and an electronics bus. The pylon is necessary to transfer the force of launch from the launch vehicle to the spacecraft. The hollow inside the pylon allows for wires, pipes and cabling to be fed through. The pylon also acts as the primary hardpoint to attach the fuel tanks, as these represent a significant portion of the mass of the spacecraft. There are two main materials that are suitable for the substructure. The 7075 aluminium alloy is commonly used in the aerospace industry due to its high specific strength.
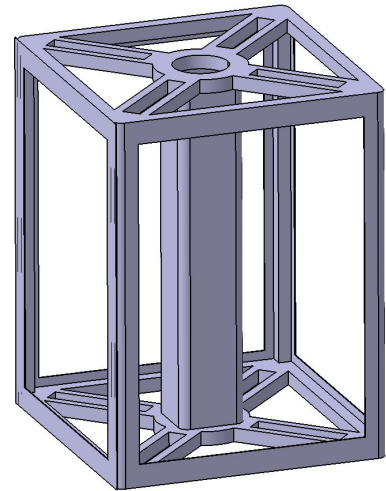
Figure 24. CAD model of spacecraft substructure.

The emerging technology however are 3D printed composite materials. Carbon fiber laced polymers can now be printed into structures which would be costly and difficult with previous casting technology. Structures like honeycomb, cubic subdivisions or gyroids provide increased specific strength additional to the material properties. To demonstrate these two types of structures and their strengths, FEA analysis has been carried out on both parts to determine the maximum displacement under the launch condition of 20G, which gives a safety factor of 2 assuming a loading of 10G at maximum acceleration. Figure 25 gives the displacement for aluminium (left) and also gives displacement for carbon fiber (right).
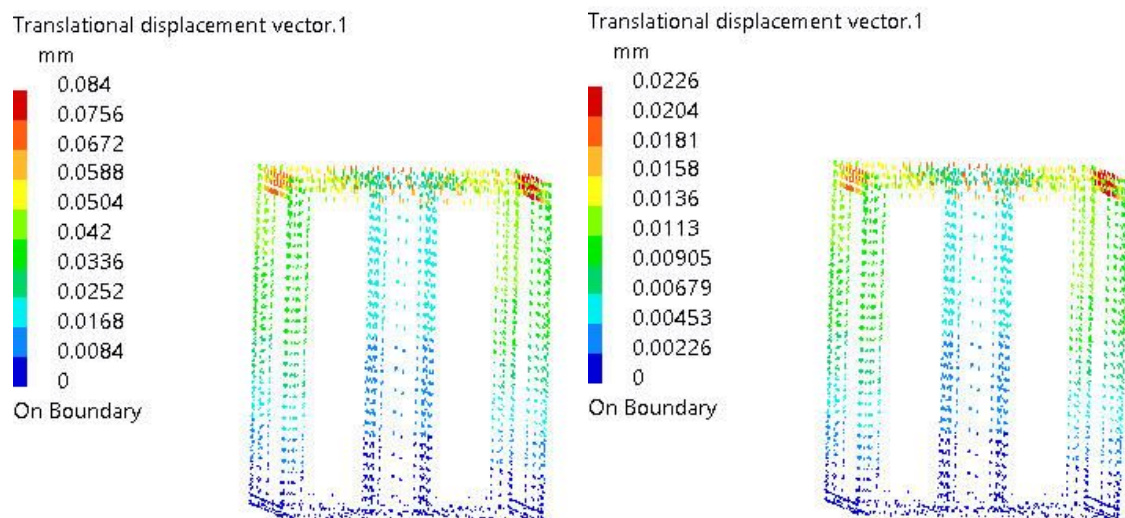
Figure 25. Structural displacement testing, aluminium vs carbon fiber.

Comparing the displacement of the two materials it can be seen that there is four-fold decrease in displacement using the printed carbon fiber material. Coupled with the weight difference of 194 kg between the aluminium and the carbon fiber, the latter becomes the more appealing choice. Though the displacement of both materials would make them both more than sufficient for the role.

The superstructure comprises the external shell and subsystem bays of the spacecraft. It has a much more varied role than the substructure. It is responsible for housing the smaller subsystems of the spacecraft; maintaining the internal thermal environment and protecting the internal hardware from debris. The superstructure is not homogenous in its material composition, instead using a variety of different materials for different roles. For example, the external surface of the superstructure is covered in the thermal covering discussed in section 3.6, the surface below that being a kevlar lining to protect the spacecraft internals from micrometeorites.

The auxiliary structures of the spacecraft are any of the various hardpoints used to attach components on the interior and exterior surfaces of the spacecraft. The majority of these hardpoints support relatively lightweight components such as the scientific instrumentation and therefore do not need to be strong. Lightweight materials are still favoured in order to keep the weight of the spacecraft as low as possible. One example of an auxiliary structure is the bracket used to secure the two NEXT-C ion thrusters to the spacecraft structure.
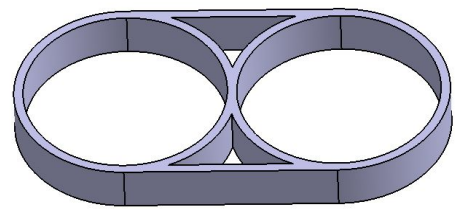

Figure 26. CAD model of thruster bracket.

As mentioned in section 3.2, the solar panels on the spacecraft use inflatable beams to stiffen the flexible panels. The use of inflatable structures in space is a keen topic of interest, having applications in solar panels, solar sails and space stations. One of the most common failures that cripple spacecraft is the failure of the solar panels to deploy. Because of the size of rigid foldable solar panels, their deployment can get complex; relying on multiple mechanical unfurling techniques. The main appeal of inflatable structures is their simplicity, but they also provide decent strength and are very lightweight. The two analyses below show the displacement of the solar panels when the spacecraft is accelerating using both ion thrusters and rotating using the attitude control system.
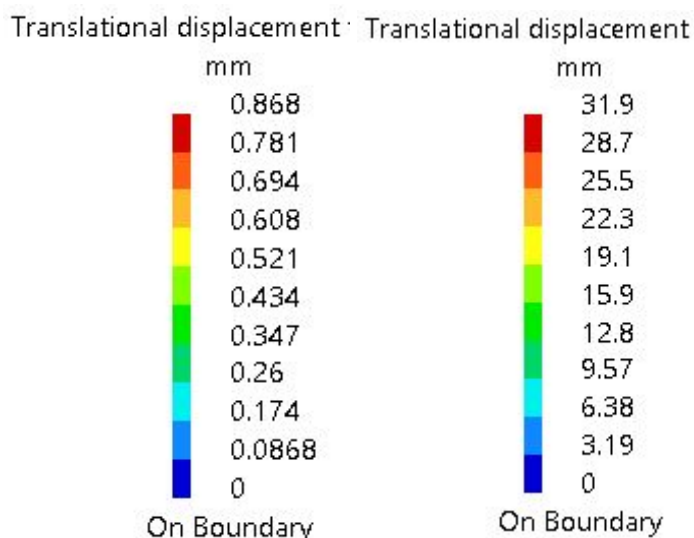

Figure 27. Structural displacement testing of the solar panels for linear and angular accelerations.

The displacement caused by the acceleration of the spacecraft is small, which makes sense considering the small acceleration caused by the low thrust ion propulsion. The rotational displacement however is much greater; though still not large enough to cause concern. 31.9mm of displacement over the 7.5 meter span of the panel shows exceptional rigidity for an inflatable structure.

The last structural component to consider is the payload adapter. This component joins the spacecraft to the launch vehicle. This means the component has to be particularly strong. A general rule of thumb for sizing the adapter is the equation $m_{LVA} = 0.0755 m_{S/C} + 50$. Figure Appendix A gives the total mass of the spacecraft as 945 kg which results in a launch vehicle adapter mass of 121 kg. The specific design of the adapter depends on the launch vehicle used and would be designed after the spacecraft as a whole.

3.8   Instruments

Careful consideration needs to be given to the scientific payload onboard the spacecraft. With limited mass and power requirements all of the instruments must either contribute to the main goal or be versatile enough to have multiple applications. The instruments utilised by past missions have been evaluated to determine their suitability to this mission, as well as techniques not yet attempted. The instruments considered for this mission are displayed below.

Selected:
- Optical camera suite.
    1. Far-field optical reconnaissance camera (FORCAM).
    2. Topology mapping camera (TOMCAM).
    3. Material acquisition and surface tracking camera (MASTCAM).
- Spectrometers.
    4. Visible and near infrared spectrometer (VINIRS).
    5. Thermal infrared emission spectrometer (TIRES).
- Altimeter.
    6. Laser ranging altimeter (LARA).
- Radar.
    7. Asteroid subsurface penetrating radar (ASP)

Rejected:
- Magnetometer.
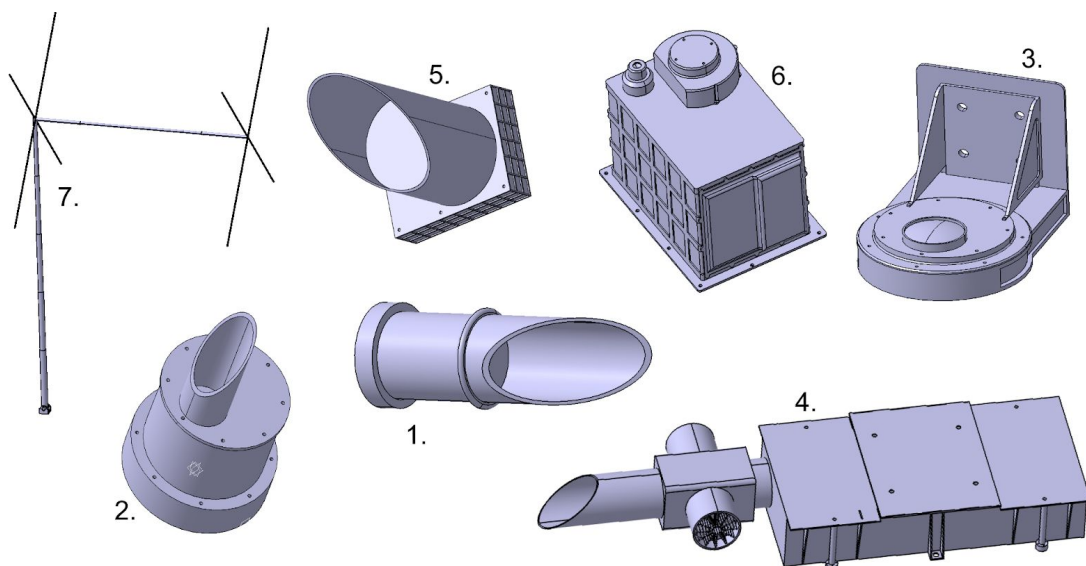- Seismometer to map asteroid crust and core (SMACC).

Figure 28. CAD models of all the scientific instruments.

FORCAM is the first instrument to acquire the asteroid while the spacecraft is still on approach. It will gather the initial images of the asteroid, increasing in resolution as the spacecraft closes in. Using a telescopic lense to image the asteroid from a distance of two million kilometers. Once situated in close proximity to the asteroid, FORCAM also functions to gather high definition images of the surface to aid in sample site selection.

TOMCAM is used to create detailed colour topological maps of the surface of the asteroid to inform the decision of sample sites. These colour images will also aid VINIRS in identifying the surface composition of the asteroid based on the colour of the emitted light.

MASTCAM provides feedback data for the sample collection, giving visual confirmation of successful maneuvers and helping to diagnose issues that may arise. It also allows for a close inspection of the asteroid surface while the maneuver is underway, further assisting the identification of sample sites. The utility of each of the instruments in the camera suite overlap to give the maximum possible data in order to find the optimum sample locations. The overlap also provides redundancy against the failure of any one instrument.

The two spectrometers onboard can be used to find the mineral and chemical composition of the asteroid, further assisting the search for sample sites. VINIRS splits the incoming light into component wavelengths which are then analysed to determine the chemical composition of the source. Each chemical and element absorbs certain wavelengths of light and emits others, these patterns can then be used to determine the chemical makeup of the source of the emitted light. This technique can be used to find organic compounds and water to aid the search for the origin of life in the Solar system. TIRES while similar to VINIRS can identify minerals constituting the asteroid. The mineral composition gives clues as to the formation of the asteroid and the early Solar system. Each mineral has its own thermal emission signature which can be analysed to determine which minerals are present and thus how they were likely formed. The minerals also reveals the potential resources contained within the asteroid.

The LARA altimeter provides the distance between the spacecraft and the asteroid. This is important when performing the sampling maneuvers so to not collide with the surface. LARA can also be used to accurately develop a model of the gravitational field of the asteroid. The mass of 4660 Nereus is not sufficient to force the material into a spheroid meaning it is not of uniform radius throughout. The mapping of the gravitational field is necessary from a navigational standpoint; but also can give clues to the internal structure of the asteroid. If there is a metallic core inside then because of its greater density the centre of gravity of the asteroid will be skewed away from the location if the asteroid were of constant density. LARA uses light detection and ranging (LIDAR) methods to bounce a laser beam from the spacecraft to the surface and back again; the time taken to return gives the range of the surface.

Radar methods can be employed in the form of a ground penetrating radar system in order to peer into the subsurface of the asteroid. ASP uses a frequency of 50 MHz as this frequency provides the best performance for the metallic minerals - such as hematite and magnetite - that are likely in high concentrations on type M asteroids. There is a balance to be made between penetration depth and resolution when choosing the operational frequency, lower frequencies give better penetration at the expense of resolution and vice-versa.

Magnetometers give data as to the magnetic fields surrounding an object. This instrument was discounted because the size of the asteroid makes it extremely unlikely that there would be an internal processes that would generate a magnetic field. Typically celestial bodies smaller than the Earth do not have the ability to generate magnetic fields. In the case of asteroids, their cores will have long since cooled, just as Mars' core has, thus no longer being able to sustain a magnetic field.

The use of a seismometer in combination with the ground penetrating radar would give a detailed model for the internal structure of the asteroid. The reason for the discounting of this instrument is the complexity that comes with its implementation. The seismometer must be fixed to the surface of the asteroid while a projectile is fired into the surface in order to generate seismic waves. These seismic waves then propagate through the internal structure and reverberate. The propagation speed of the waves depends on the material they are travelling

through and this is the method by which the interior structure is mapped. As stated this method would require two independant ancillary probes which increases the complexity greatly.

3.9   Sample Collection[23]

Collecting samples from the surface of the asteroid is the main objective of the mission and therefore of the highest importance. In order to determine the most efficient methods to sample the asteroid, real life examples can provide valuable insights to adopt or adapt to suit the purpose. The examples fall into two categories, Earth based sampling and the methods used by previous sample return spacecraft. Typically on Earth, the sampling methods usually take the form of core drilling. These cores of material have uses ranging from the oil industry, paleontology and civil engineering. Core drills are typically variations of hollow cylinders with peg-like 'teeth', with the core sample being fed into the centre of the cylinder as the drill 'bites' into the material. Harder materials such as those found in reinforced concrete buildings or on a metallic asteroid require harder drill bits that can be provided by steel. Artificial diamonds can be embedded into the steel teeth which -owing to their exceptional hardness- protect the bit from the abrasion of the drilling medium.

The three previous asteroid sample return missions used novel techniques to sample their respective asteroids. The Hayabusa missions using a kinetic projectile to eject particulates into a cone, funneling them into the collector. Alternatively the OSIRIS-REx mission uses compressed nitrogen gas to eject the particulates. These methods both rely on the sample medium being loosely scattered on the surface of the asteroid. Any attempt at sampling the subsurface requires an impactor to remove the upper surface. This would release potentially large particulates from the surface which may damage the spacecraft.

This spacecraft will use two sampling methods, one to sample the surface regolith and another to sample the subsurface. The spacecraft will utilise a robotic arm similar to OSIRIS-REx to maneuver the sampling devices. This is in an effort to prevent a failure similar to the original Hayabusa mission, where the sample horn attached to the bottom of the spacecraft collided with the surface. Samples of the regolith were still obtained, albeit at smaller than expected amounts. Having the samplers on the arm gives a greater level of control and precision when maneuvering them. The arm can be seen in its stowed configuration below.
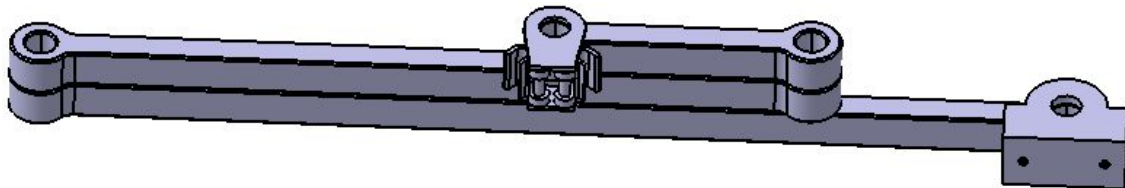

Figure 29. CAD model of robotic arm in stowed configuration.

The length of the arm is sufficient to be able to deposit the samples into the return capsule located at the front of the spacecraft. The arm utilises a device similar to the quickloader for excavators, except using two hooks instead of just one. This mechanism allows the swapping between the two samplers without needing a second arm. This can be seen in figure 30.
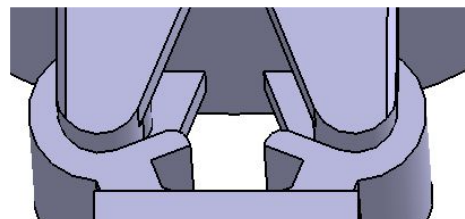

Figure 30. Connector mechanism between robot arm and sample devices.

The regolith sampler will build upon the Hayabusa method of using a kinetic projectile. A tungsten bullet will be used as the projectile as it is dense and hard to aid with penetration depth and momentum transfer to the surface regolith.

This method was chosen because although seemingly more complex, does not require extra mass in the form of compressed nitrogen or complexity associated with the feed systems. The design models of the sampler named the repeating kinetic projectile sampler (ReKiPs) is shown below. The revolving cylinder (figure 31) has four sample capsules and projectiles corresponding to four surface samples. The revolving cylinder allows for the samples taken from multiple sites to remain separate for analysis.
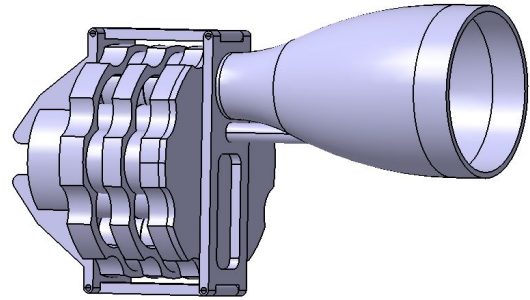

Figure 31. CAD model of ReKiPs sampler.

Once all the samples have been collected the muzzle of ReKiPs can be opened so that the whole cylinder can be placed inside of the sample return re-entry vehicle (SAREV). The front plate is attached to the cylinder but does not rotate along with it, this means that when the cylinder rotates, the capsule previously exposed is sealed, and another is exposed ready for another sample. The rear of the cylinder has space to store four core samples from the next sampler which will be discussed next.
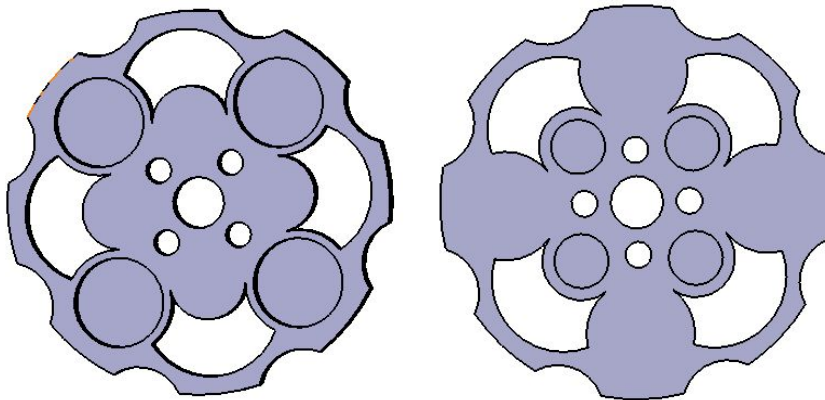

Figure 32. CAD models of the front and back of the cylinder.

The second sampler named the diamond tipped subsurface core drill (Discord) uses a diamond tipped core drill in order to acquire samples of the asteroid subsurface. There are problems associated with using a rotary drill on the surface of an asteroid that must be overcome. Firstly, the friction causes the heating of the drill bit, this can cause warping and damage to the bit. On Earth this is solved by using a coolant to remove the excess heat. However the density of the coolant and the amount required prohibits this solution for spacecraft; as well as the risk of contaminating the sample. One possible solution would be to create internal cooling passages to pump coolant in a sealed system. This is feasible, but would require extensive analysis to determine the optimum balance between structural strength and cooling. The easiest solution to implement is to reduce the size and power of the drill, as the larger the surface area, the larger the frictional force. Spinning the bit slower, while taking longer to complete the sampling, will reduce the friction coefficient and therefore the heat transfer. The design model of Discord is displayed below.
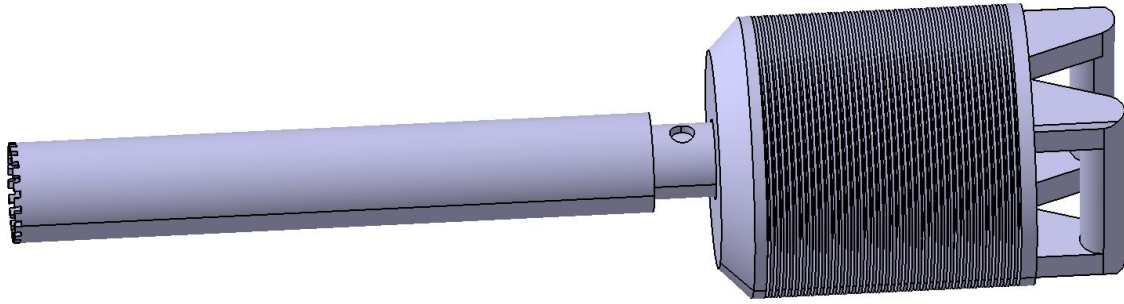
Figure 32. CAD model of Discord sample device.

The second problem facing the successful implementation of a rotating drill is the torque from the motor. As the spacecraft will be floating when the drill is in operation there is nothing to brace it against. Due to the conservation of angular momentum, when the drill begins to spin, the spacecraft will rotate in the opposite direction. This too can be overcome by making use of a system already fitted to the spacecraft; the momentum wheels. If once the drill begins to spin, the momentum wheels begin to spin in the opposite direction with equal angular momentum then the spacecraft will remain motionless. The only requirement is that the torque produced by the drill not exceed the maximum torque available from the wheels. A small diameter drill bit spinning at low speed will not have the required torque to overcome the reaction wheels; this is another reason to keep the speed and size of the drill small. The third problem is how to 'snap' the core from the asteroid when the drill has reached maximum depth. Core drilling in industrial applications usually drills through a material and to the other side, eliminating the need to snap the core. In the event of a sample that does not emerge on the other side, a brute force method is used to dislodge the core. The resolution of this problem comes courtesy of the Apollo space program [23], where core drills were used on the Moon by astronauts. These drills functioned as similar to jackhammers, as well as rotating they also forcibly hit downwards. This method breaks the core into smaller slices which stay inside the drill bit until retrieved. Discord has a ramrod design built in that pushes the core out of the bit when required. After a sample is collected, the bit is positioned over the sample return pod and the core is pushed out of the bit by the ramrod and into the awaiting core capsule. Once all four cores are placed into the SAREV return capsule the lid is closed, sealing the samples to prevent foreign contamination on re-entry and recovery. The section below discusses how these samples are safely returned to the planet.

3.10 Sample Return

This section will discuss the method by which the samples are returned back to Earth from the asteroid. The samples must survive atmospheric re-entry while remaining unspoiled and uncontaminated. In order to achieve this goal the samples must have a protective vessel capable of safely passing through the atmosphere and landing at a suitable site for retrieval. The hypersonic velocities which the vehicle will re-enter with result in extreme temperatures that would melt most metals. Therefore high temperature materials and vehicle geometries must be employed to prevent the destruction of the vehicle and the samples along with it. There are very few materials capable of surviving the temperatures of atmospheric re-entry, one highly successful technique is to use a material that is intentionally designed to be destroyed. These are ablative materials and they function by using the vaporisation of the material to create a thin layer of gas separating the structure and the hot gasses of the atmosphere; this is known as a boundary layer.
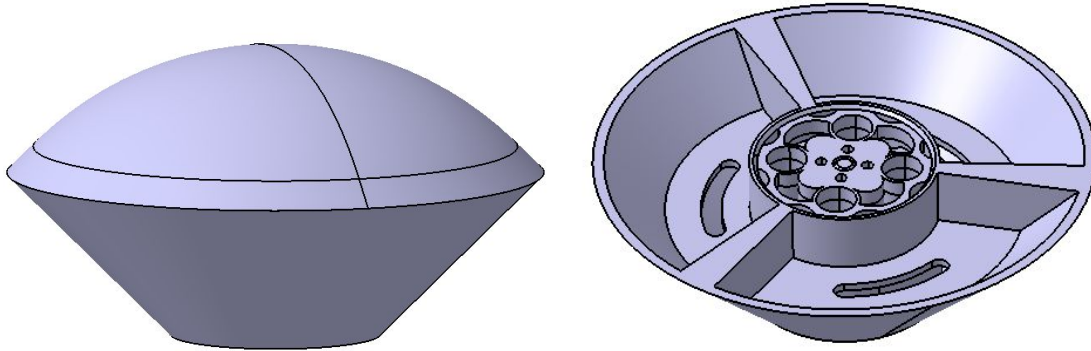
Figure 33 (left) and 34 (right) shows the CAD models for the return capsule with and without the lid.

Figure 33 shows the closed capsule ready for re-entry and figure 34 shows the capsule with the lid removed to see inside. There is space for three parachutes at 120 degree spacing, with areas underneath the parachutes to house the electronics. The central core houses the samples inside the revolver core. There is a secondary lid inside the capsule which when shut forms a seal to protect the samples. The top lid of the capsule is coated in ablative material and is shaped such as to create a cushion of cooler air between the hot gasses and the capsule.

The capsule departs the spacecraft when the trajectory sets it to re-enter the Earth's atmosphere. Once departed the spacecraft maneuvers to avoid the atmosphere while the capsule enters the atmosphere. The capsule uses the atmospheric drag to slow itself down to the point where it can blow off the top lid and deploy the three parachutes. Once the capsule lands on the surface it can be retrieved and opened in a controlled environment so to not contaminate the samples. The entire way down to the surface the capsule is communicating with the ground, providing telemetry and positional data. In the event of a parachute failure, two of the three parachutes is enough to slow the capsule.

4. ASSEMBLY & EVALUATION

Now that all the subsystems of the spacecraft have been designed they can be assembled together. Naturally the placement of the components in relation to each other is crucial, the robotic arm for example must be placed within reach of the sample return capsule. With all the components designed, the spacecraft mass can be calculated. Appendix A gives the mass values for each of the components. The calculated total dry mass of the spacecraft is 766 kg. With this value the fuel needed can then be calculated. For the delta V of 6 Km/s necessary for the return journey the propellant mass is 120 kg. Multiplying this by 1.5 to give extra redundancy fuel gives a total propellant mass of 180 kg. Bringing the spacecraft wet mass up to 945 kg. Factoring in the launch vehicle adapter at 121 kg gives a launch mass of 1066 kg, placing it between the Hayabusa2 at 609 kg at launch and OSIRIS-REx at 2110 kg.

This launch mass is well within the stated limits for the launch set out in section 2.2. As this is a conceptual design, mass creep must be considered. Mass creep is the tendency for the mass of spacecraft to increase from initial concept to launchpad. The value of mass creep can be as much as 30% meaning in order to account for this the launch mass needs to be made 30% heavier, giving a upper bound estimate of 1387 kg. Despite this, the spacecraft is still within the mass limit to be launched from all available launchers. In fact, the spacecraft mass creep would have to be 287% of the conceptual mass in order to not be launchable on even one of the rockets.

The assembly created in this report is illustrative only, the detail needed for a full assembly model lies outside of the scope of a conceptual design. The designs on page 37 show how the spacecraft looks when assembled, more detailed design drawings can be found in appendix B.
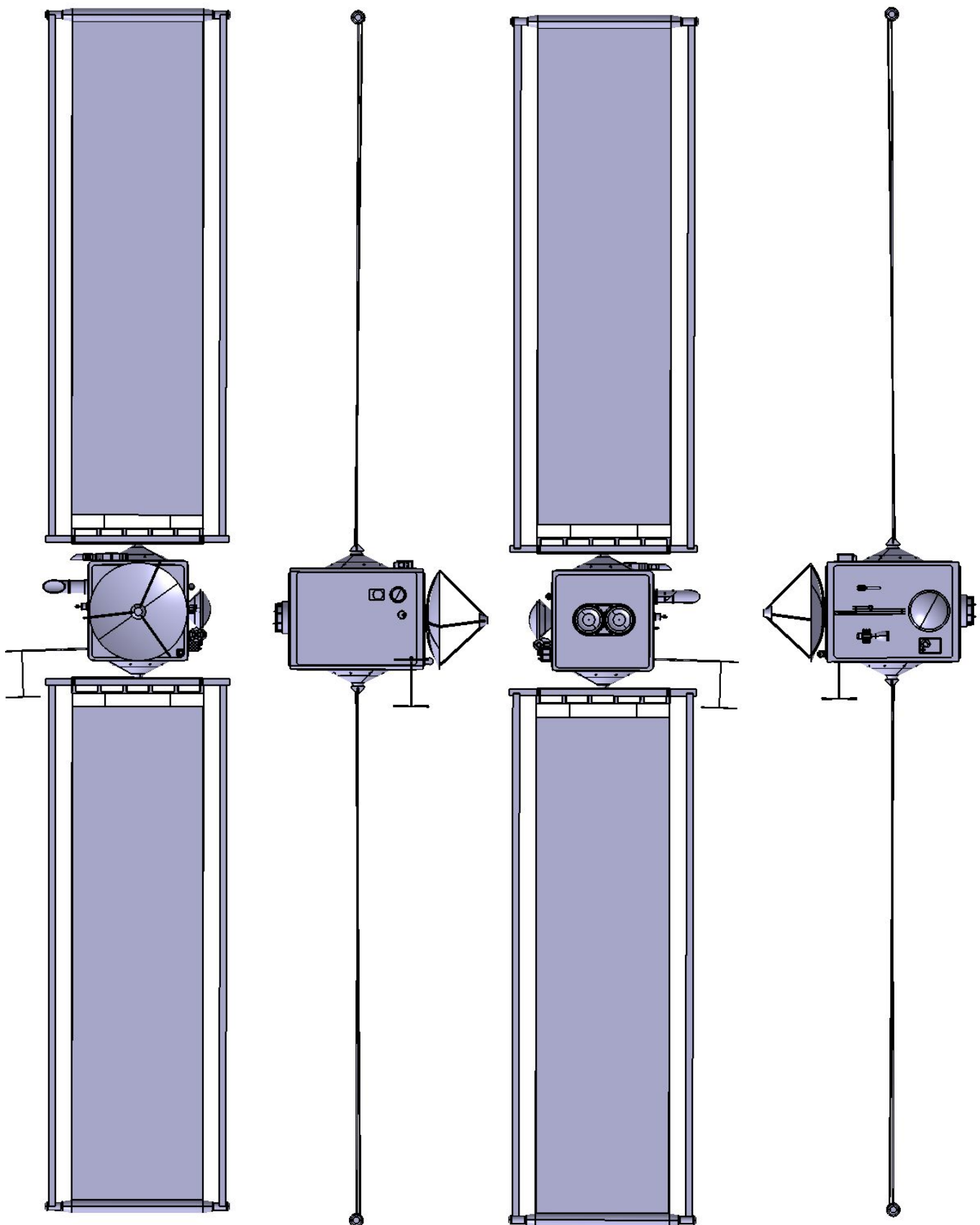
Figure 35. CAD models for the spacecraft assembly.

The evaluation of the spacecraft needs to be looked at from a global perspective to judge its suitability to the role. This is due to the iterative nature of the subsystem design, meaning that the subsystems all fit their respective roles because if they didn't then they were redesigned. This approach makes sense because of the dependencies of the subsystems on each other; if one subsystem had to be redesigned then other subsystems would have to be redesigned also. There are two main questions to ask to determine whether the spacecraft fits the mission profile. Firstly, does it have a method of sampling the spacecraft and returning those samples. And secondly do the other subsystems enable the spacecraft to achieve the this. As is discussed in section 3.9 and 3.10 the spacecraft is well equipped to achieve sample collection and return. The subsystems of the spacecraft all function within acceptable ranges and provide it with the means to travel to 4660 Nereus and return, while maintaining samples and scientific instruments.

5.   CONCLUSION

At the close of this report, the case must be presented for the feasibility of this design. One advantage of the design is that it uses proven technology, the sampling systems having been used in industry and by other spacecraft. Wherever technology has been used that has not been flight tested, the testing that has been done is extensive; the NEXT-C thruster for example has not yet flown a mission, but has been tested for continual operation over a period of years without failure. All this means that the systems onboard the spacecraft are reliable and entirely feasible with current technology.

Furthermore the tables in appendix A show that the spacecraft is well within the requirements both in terms of total takeoff mass and power consumption. If either of those were close to the limits then the balancing of the spacecraft would become difficult and any changes may become impossible to implement. There is sufficient gap between the value and upper bounds to allow for the increasing of the mission scope should that become desired further down the development process.

5.1   Further Development

The natural progression of the project from this point is to create a team of people to flesh out the designs. The analysis done in this report shows that the methods work, the next step is to optimise them. The design will likely change between the conceptual designs proposed by this report and the ready to launch vehicle. Every effort has been made to provide redundancy to allow for failures and changes to the design.

The addition of ancillary probes would give the spacecraft even more flexibility, enabling the use of seismographs to map the internal structure and establish a permanent lander on the surface. These probes were too time consuming to design and test during the timeframe, but with additional time there is no reason why they could not be included.

Analysis on the reentry vehicle to determine whether it can survive reentry and the optimum shape required to do so would have been a key design requirement; were it not for the complexity involved in hypersonic flow modelling. Going forward with additional time, this analysis should be performed to optimise the geometry of the reentry vehicle.

Determining trajectories for the spacecraft to take, both outbound and return, required extensive and complicated simulations which would again not be feasible. With more time they could be done not just for the proposed mission plan, but also to plan for missed transfer windows and other problems that may arise. More complex maneuvers such as gravity assists could be calculated to reduce the fuel required. If the maneuvers for the main mission are made efficient enough then the excess fuel could be used for a 'small body tour' of the solar system.

6.   PROJECT MANAGEMENT REVIEW

In this section the management of the project from start to finish will be shown, including the deviations from the original project timeline. Initially the timeline of the project was based heavily on the design lifecycle, however this turned out to be a far too linear view of the work when in fact the design processes were more iterative and there were far more dependencies than indicated in the original plan. Figure 36 shows the Gantt chart used to plan the project timeline and figure 37 shows how this Gantt chart evolved into its current form at the closure of the project.
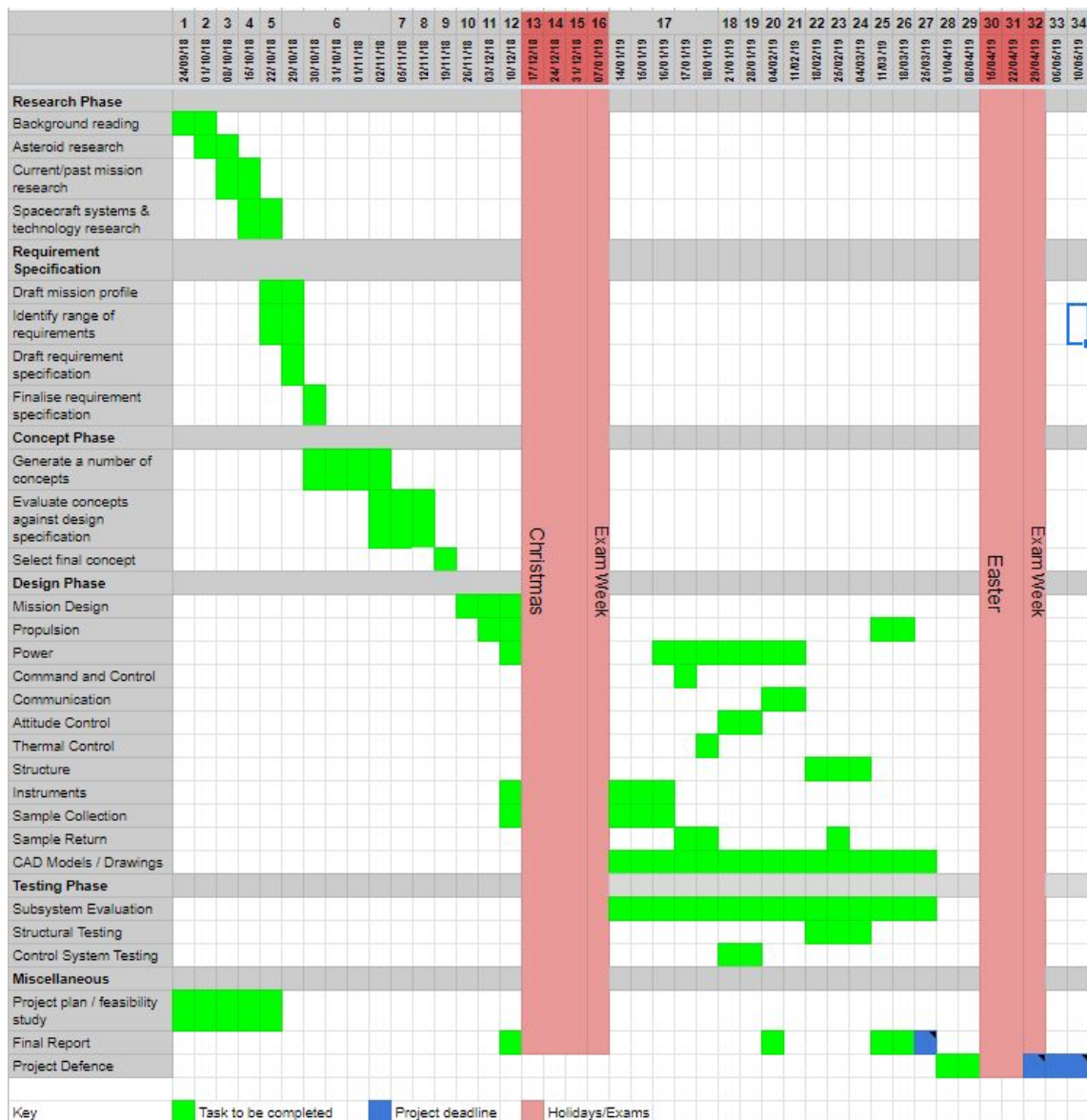

Figure 36. Original Gantt chart.

Figure 37. Gantt chart showing the actual progression of the project.

As can be seen, there are vast differences between the two Gantt charts during the design phase. The design of many subsystems was dependent on one or multiple other subsystems being designed first. Some of them has to be paused and resumed once other subsystems were designed. The testing phase which was originally intended to take place after the design phase instead ran parallel with it, forming an iterative design process. The subsystem was designed then tested, if the design was insufficient to fulfil the task then it was redesigned and tested again. This repeated until a design was found that met the criteria and passed the tests. Because of the dependent nature of many of the subsystems on each other, the later redesign of one subsystem meant the redesign of many. Using an iterative design process made sure that the part is fit for task before moving onto the next.

7. REFERENCES

1. N. Todd, "Lunar Rocks and Soils from Apollo Missions", *Curator.jsc.nasa.gov*, 2019. [Online]. Available: https://curator.jsc.nasa.gov/lunar/. [Accessed: 19- Mar- 2019].

2. S. Fornasier, B. Clark and E. Dotto, "Spectroscopic survey of X-type asteroids", Icarus, vol. 214, no. 1, pp. 131-146, 2011. Available: 10.1016/j.icarus.2011.04.022.

3. S. Fornasier, B. Clark, E. Dotto, A. Migliorini, M. Ockert-Bell and M. Barucci, "Spectroscopic survey of M-type asteroids☆", Icarus, vol. 210, no. 2, pp. 655-673, 2010. Available: 10.1016/j.icarus.2010.07.001.

4. D. Herman, G. Soulas, J. Van Noord and M. Patterson, "NASA's Evolutionary Xenon Thruster (NEXT) Long-Duration Test Results", *Journal of Propulsion and Power*, vol. 28, no. 3, pp. 625-635, 2012. Available: 10.2514/1.b34321.

5. G. Schmidt, M. Patterson and S. Benson, "THE NASA EVOLUTIONARY XENON THRUSTER (NEXT): THE NEXT STEP FOR U.S. DEEP SPACE PROPULSION", *Ntrs.nasa.gov*, 2008. [Online]. Available: https://ntrs.nasa.gov/archive/nasa/casi.ntrs.nasa.gov/20080047732.pdf.

6. M. Patterson and S. Benson, "NEXT Ion Propulsion System Development Status and Performance", *43rd AIAA/ASME/SAE/ASEE Joint Propulsion Conference & Exhibit*, 2007. Available: 10.2514/6.2007-5199.

7. G. Dudley and J. Verniolle, "Secondary Lithium Batteries for Spacecraft", *Esa.int*, 1997. [Online]. Available: http://www.esa.int/esapub/bulletin/bullet90/b90dudle.html.

8. T. McMahan, "Inflatable Solar Array Technology Packs Incredible Power In Small Pack", *NASA*, 2014. [Online]. Available: https://www.nasa.gov/centers/marshall/news/news/releases/2014/14-112.html.

9. L. Johnson, L. Fabisinski, K. Cunningham and S. Justice, "Lightweight Inflatable Solar Array: Providing a flexible, efficient solution to space power systems for small spacecraft", 2014.

10. A. Ulvestad, "A Brief Review of Current Lithium Ion Battery Technology and Potential Solid State Battery Technologies", 2018.

11. National Aeronautics and Space Agency, "Handbook of space-radiation effects on solar-cell power systems.", Clearinghouse, 1994.

12. C. Keesee, "Spacecraft Computer Systems", Michigan Institute of Technology, 2003.

13. M. Sabbadini, "Antenna design for Space Applications", Noordwijk, The Netherlands, 2009.

14. K. Satish Kumar, "Design and Analysis of Parabolic Reflector Using MATLAB", International Journal of Advanced Research in Electrical, Electronics and Instrumentation Engineering, vol. 04, no. 03, pp. 1367-1373, 2015. Available: 10.15662/ijareeie.2015.0403029.

15. P. Bevelacqua, "Antenna-Theory.com - Parabolic Dish Reflector Antenna (Page 2)", Antenna-theory.com. [Online]. Available: http://www.antenna-theory.com/antennas/reflectors/dish3.php.

16. R. Snider, "Attitude Control of a Satellite Simulator Using Reaction Wheels and a PID Controller", Postgraduate Masters, Air Force Institute of Technology, 2010.

17. A. Tewari, Atmospheric and space flight dynamics. Boston: Birkhäuser, 2007.

18. "High Motor Torque Momentum and Reaction Wheels", Rockwellcollins.com, 2016. [Online]. Available: https://www.rockwellcollins.com/Products-and-Services/Defense/Platforms/Space/High-Motor-Torque-Momentum-and-Reaction-Wheels.aspx.

19. P. Chandrasekhar et al., "Variable-emittance infrared electrochromic skins combining unique conducting polymers, ionic liquid electrolytes, microporous polymer membranes, and semiconductor/polymer coatings, for spacecraft thermal control", Journal of Applied Polymer Science, vol. 131, no. 19, p. n/a-n/a, 2014. Available: 10.1002/app.40850.

20. A. Le van and C. Wielgosz, "Finite element formulation for inflatable beams", Thin-Walled Structures, vol. 45, no. 2, pp. 221-236, 2007. Available: 10.1016/j.tws.2007.01.015.

21. D. Li, W. Liao, N. Dai, G. Dong, Y. Tang and Y. Xie, "Optimal design and modeling of gyroid-based functionally graded cellular structures for additive manufacturing", Computer-Aided Design, vol. 104, pp. 87-99, 2018. Available: 10.1016/j.cad.2018.06.003.

22. "Gyroid infill tests", Laplacean, 2018. [Online]. Available: https://laplacean.wordpress.com/2018/05/17/gyroid-infill-tests/. [Accessed: 29- Mar- 2019].

23. K. McNamara et al, "Concepts and benefits of lunar core drilling.", NASA, Houston, 2019.

8. BIBLIOGRAPHY

1. G. D'Eleuterio and P. Baines, Elements of spacecraft design. [Toronto]: University of Toronto, Faculty of Applied Science and Engineering, 1987.

2. A. Banday, S. Zaroubi and M. Bartelmann, Mining the Sky. Berlin: Springer Berlin, 2014.

3. C. Kowal, Asteroids: their nature and utilization. New York: John Wiley, 1996.

4. R. Humble, G. Henry and W. Larson, Space propulsion analysis and design. New York: McGraw-Hill, 2007.

5. Dunn JJ, Hutchison DN, Kemmer AM, Ellsworth AZ, Snyder M, White WB, Blair BR. 3D printing in space: enabling new markets and accelerating the growth of orbital infrastructure. Proc. Space Manufacturing. 2010 Oct;14.

6. L. Adams, Technology for small spacecraft. Washington, D.C.: National Academy Press, 1994.

7. T. Sarafin and W. Larson, Spacecraft structures and mechanisms. Hawthorne, Calif.: New York, N.Y., 2007.

8. P. Fortescue, J. Stark and G. Swinerd, Spacecraft systems engineering.

9. A. Tewari, Atmospheric and space flight dynamics. Boston: Birkhäuser, 2007.

10. "JPL Solar System Dynamics", Ssd.jpl.nasa.gov, 2019. [Online]. Available: https://ssd.jpl.nasa.gov.

11. M. Morimoto, H. Yamakawa, M. Yoshikawa, M. Abe and H. Yano, "Trajectory design of multiple asteroid sample return missions", Advances in Space Research, vol. 34, no. 11, pp. 2281-2285, 2004. Available: 10.1016/j.asr.2003.10.055.

12. Y. Tsuda, M. Yoshikawa, M. Abe, H. Minamino and S. Nakazawa, "System design of the Hayabusa 2—Asteroid sample return mission to 1999 JU3", Acta Astronautica, vol. 91, pp. 356-362, 2013. Available: 10.1016/j.actaastro.2013.06.028.

13. I. Nakatani, M. Hashimoto, H. Saito, M. Kamimura and M. Adachi, "Advanced spacecraft design for asteroid sample return mission", Acta Astronautica, vol. 35, pp. 231-238, 1995. Available: 10.1016/0094-5765(94)00188-r.

14. K. NISHIYAMA, S. HOSODA, K. UENO, R. TSUKIZAKI and H. KUNINAKA, "Development and Testing of the Hayabusa2 Ion Engine System", TRANSACTIONS OF THE JAPAN SOCIETY FOR AERONAUTICAL AND SPACE SCIENCES, AEROSPACE TECHNOLOGY JAPAN, vol. 14, no. 30, pp. Pb_131-Pb_140, 2016. Available: 10.2322/tastj.14.pb_131.

15. A. Tewari, Atmospheric and space flight dynamics. Boston: Birkhäuser, 2007.

16. "Spacecraft Overview – New Horizons", Spaceflight101.com, 2019. [Online]. Available: http://spaceflight101.com/newhorizons/spacecraft-overview/.

17. "Hayabusa 2", Spaceflight101. [Online]. Available: http://www.spaceflight101.net/hayabusa-2.html.

18. E. arXiv, "Asteroid mining might actually be better for the environment", MIT Technology Review, 2018. [Online]. Available: https://www.technologyreview.com/s/612311/asteroid-mining-might-actually-be-better-for-the-environment/.

9.   APPENDIX A

Subsystem	Power Draw
Propulsion	
Power Processing Unit	7,000.00 W
NEXT-C Propulsor	6,900.00 W
Communication	
High Gain Antenna	100.00 W
Low Gain Antenna #1	35.00 W
Low Gain Antenna #2	35.00 W
Scientific Payload	
PolyCam	5.30 W
Optical Cam	5.30 W
MapCam	5.30 W
Laser Altimeter	17.00 W
Thermal Spectrometer	30.00 W
Visible & Infrared Spectrometer	30.00 W
Command and Control	
Experiment Control Computer	20.00 W
Flight Data and Diagnostics Computer	20.00 W
Guidance Computer	20.00 W
Command Computer	20.00 W
Thermal Control	
Heaters (High)	4,800.00 W
Heaters (Low)	1,500.00 W

Variable Emittance Skin	12.00 W
Attitude Control	
Momentum Wheels Nominal	22.00 W
Momentum Wheels Max	90.00 W
RCS Thrusters	2.20 W
Sample Collection	
Drill	430.00 W
Max during cruise	14.12 kW
Total without thrusters	899.10 W

Power draw table.

Component	Mass	Percentage
Propulsion		
NEXT-C Thruster 1	13.50 kg	1.43%
NEXT-C Thruster 2	13.50 kg	1.43%
Propellant	179.32 kg	18.97%
Power		
Solar Panel 1	33.28 kg	3.52%
Solar Panel 2	33.28 kg	3.52%
Batteries	36.00 kg	3.81%
Power Supply Unit	79.88 kg	8.45%
Science Payload		
PolyCam	5.00 kg	0.53%
Optical Cam	0.60 kg	0.06%
MapCam	0.60 kg	0.06%
Laser Altimeter	3.70 kg	0.39%
Thermal Spectrometer	6.00 kg	0.63%
Visible & Infrared Spectrometer	9.80 kg	1.04%

Communication		
High Gain Antenna	35.00 kg	3.70%
Low Gain Antenna 1	1.20 kg	0.13%
Low Gain Antenna 2	1.20 kg	0.13%
Communication Electronics (Amplifiers, Converters, Multiplexers)	30.00 kg	3.17%
Command and Control		
Experiment Control Computer	5.00 kg	0.53%
Flight Data and Diagnostics Computer	5.00 kg	0.53%
Guidance Computer	5.00 kg	0.53%
Command Computer	5.00 kg	0.53%
Thermal Control		
Electrochromatic Skin	28.80 kg	3.05%
Attitude Control		
Reaction Wheel 1	7.70 kg	0.81%
Reaction Wheel 2	7.70 kg	0.81%
Reaction Wheel 3	7.70 kg	0.81%
RCS Propellant	50.00 kg	5.29%
16x RCS Thrusters	32.00 kg	3.39%
Structure		
Spacecraft Substructure	207.00 kg	21.90%
Spacecraft Superstructure	75.00 kg	7.93%
Miscellaneous Components		
Wires, Fasteners and Paints	27.53 kg	2.91%
Launch Mass		
Spacecraft	945.29 kg	
Launch Vehicle Adapter	121.37 kg	

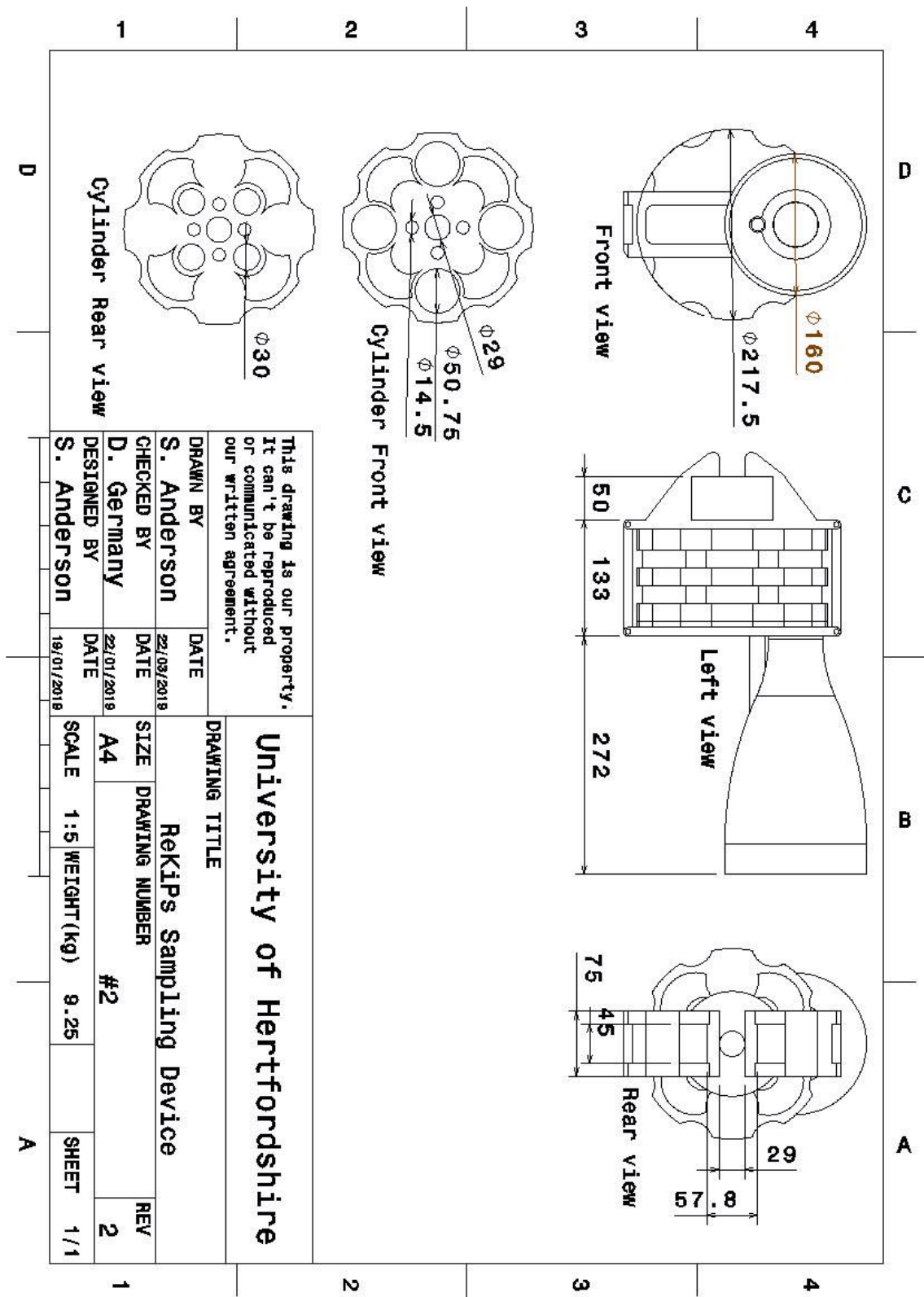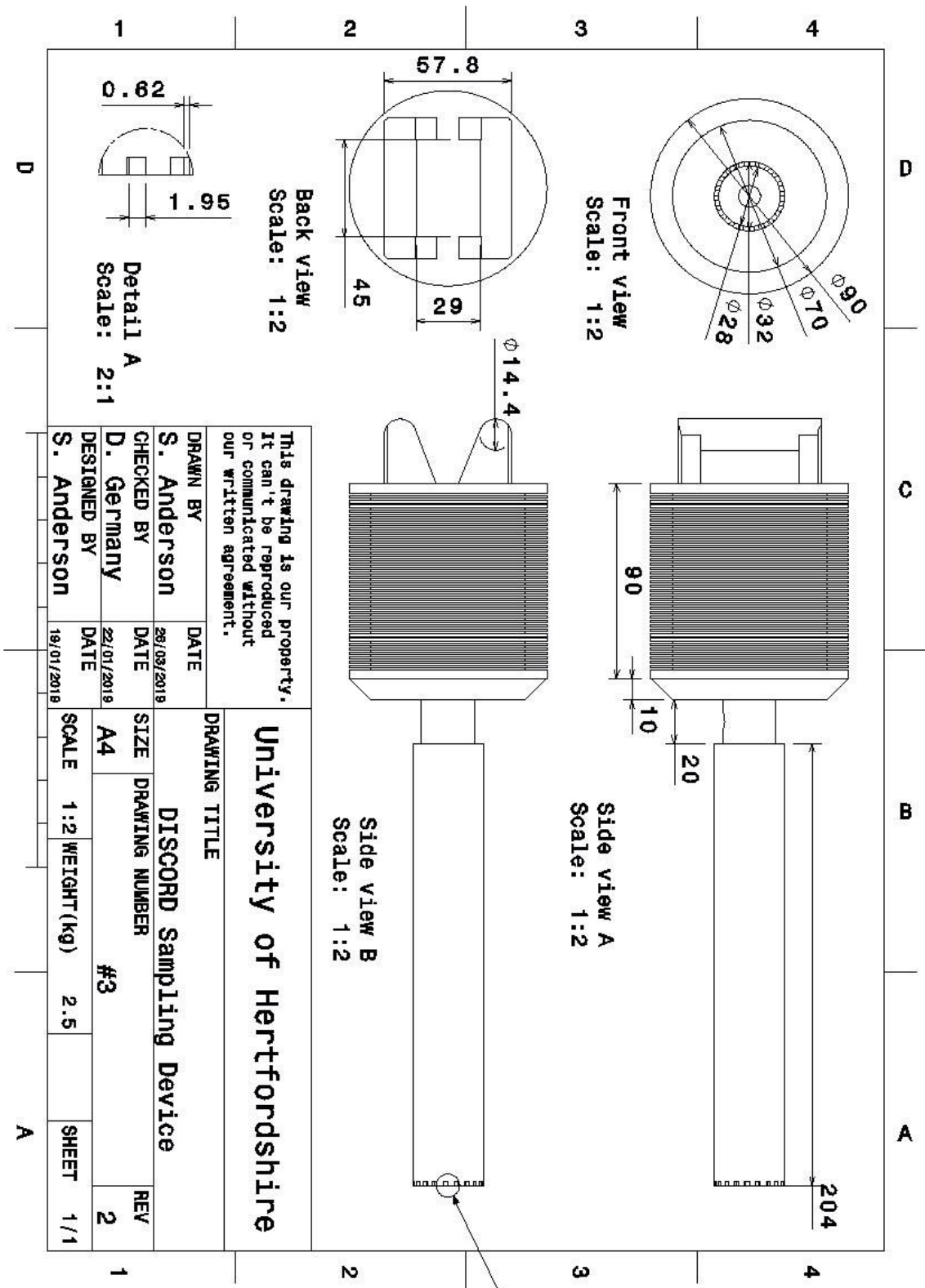| Total Launch Mass	1,066.66 kg	

Mass breakdown table.

10. APPENDIX B
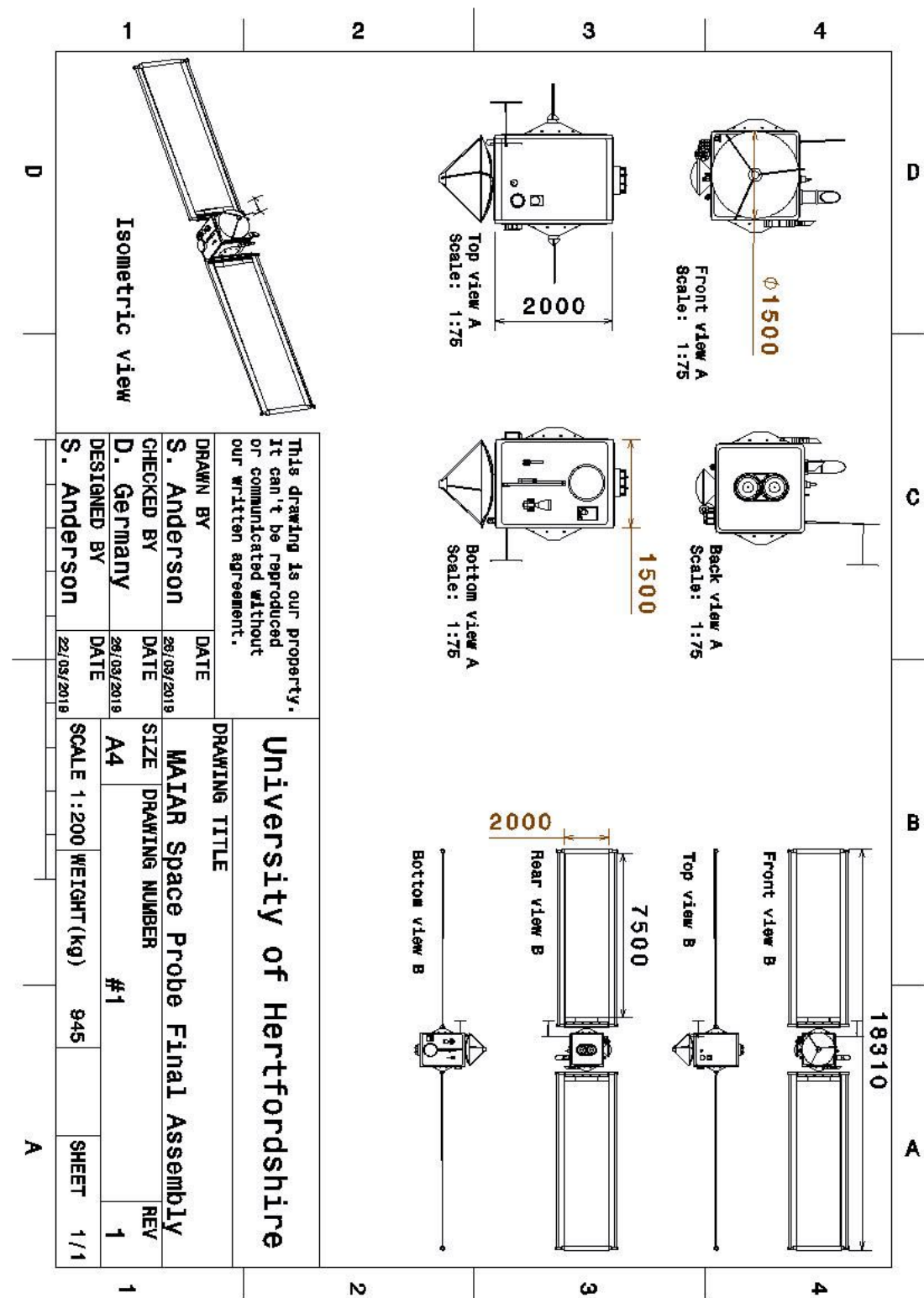
Assembly drawing.

ReKiPs sampler drawing.

DISCORD sample device.